Redox Biology 37 (2020) 101751

Contents lists available at ScienceDirect

Redox Biology

journal homepage: www.elsevier.com/locate/redox

Research Paper

# Diclofenac impairs autophagic flux via oxidative stress and lysosomal dysfunction: Implications for hepatotoxicity

Seung-Hwan Jung [a], Wonseok Lee [a], Seung-Hyun Park [a], Kang-Yo Lee [a], You-Jin Choi [a], Soohee Choi [b], Dongmin Kang [b], Sinri Kim [c], Tong-Shin Chang [a], Soon-Sun Hong [d], Byung-Hoon Lee [a,*]

[a] College of Pharmacy and Research Institute of Pharmaceutical Sciences, Seoul National University, 1 Gwanak-ro, Gwanak-gu, Seoul, Republic of Korea
[b] Department of Life Science, Ewha Womans University, 52 Ewhayeodae-gil, Seodaemun-gu, Seoul, Republic of Korea
[c] Graduate School of Pharmaceutical Sciences, Ewha Womans University, 52 Ewhayeodae-gil, Seodaemun-gu, Seoul, Republic of Korea
[d] Department of Biomedical Sciences, College of Medicine, Inha University, Sinheung-dong, Jung-gu, Incheon, 400-712, Republic of Korea

ARTICLE INFO

*Keywords:*
Diclofenac
Hepatotoxicity
Lysosomal dysfunction
Mitophagy
Nonsteroidal anti-inflammatory drugs
Reactive oxygen species

ABSTRACT

Treatment with nonsteroidal anti-inflammatory drugs (NSAIDs) is associated with various side effects, including cardiovascular and hepatic disorders. Studies suggest that mitochondrial damage and oxidative stress are important mediators of toxicity, yet the underlying mechanisms are poorly understood. In this study, we identified that some NSAIDs, including diclofenac, inhibit autophagic flux in hepatocytes. Further detailed studies demonstrated that diclofenac induced a reactive oxygen species (ROS)-dependent increase in lysosomal pH, attenuated cathepsin activity and blocked autophagosome-lysosome fusion. The reactivation of lysosomal function by treatment with clioquinol or transfection with the transcription factor EB restored lysosomal pH and thus autophagic flux. The production of mitochondrial ROS is critical for this process since scavenging ROS reversed lysosomal dysfunction and activated autophagic flux. The compromised lysosomal activity induced by diclofenac also inhibited the fusion with and degradation of mitochondria by mitophagy. Diclofenac-induced cell death and hepatotoxicity were effectively protected by rapamycin. Thus, we demonstrated that diclofenac induces the intracellular ROS production and lysosomal dysfunction that lead to the suppression of autophagy. Impaired autophagy fails to maintain mitochondrial integrity and aggravates the cellular ROS burden, which leads to diclofenac-induced hepatotoxicity.

## 1. Introduction

Nonsteroidal anti-inflammatory drugs (NSAIDs) are one of the most commonly used analgesic and anti-inflammatory agents worldwide. However, they are associated with various side effects, including gastrointestinal, cardiovascular, renal and hepatic disorders. Some NSAIDs have been withdrawn from the market due to fatal cardiovascular and hepatic toxicity. A systematic analysis of the data collected in the Drug-Induced Liver Injury Network revealed that diclofenac is the NSAID most frequently implicated in hepatocellular injury development [1]. Mitochondria are the central organelles responsible for diclofenac-induced hepatotoxicity. Diclofenac and its reactive metabolites induce apoptosis in human and rat hepatocytes by altering mitochondrial function and generating reactive oxygen species (ROS) [2,3]. They also inhibit oxidative phosphorylation and ATP synthesis in rat liver mitochondria [4]. While mitochondria are the major site of hepatic ROS production induced by diclofenac, the expression of NADPH oxidase (NOX) and the NOX-dependent generation of superoxide anion were also increased markedly by diclofenac in other tissues [5,6].

Autophagy is a homeostatic process that induces the recycling of intracellular materials under conditions of various cellular stresses. The relationship between ROS and autophagy is complex. At low concentrations, ROS serve as signaling molecules for cell growth and survival. Under nutrient starvation conditions, cells produce ROS and oxidize ATG4 that is essential for the initiation of autophagosome formation [7]. ROS also induce autophagy indirectly by activating AMPK or by releasing Atg6/Beclin 1 from suppression by Bcl-2 [8,9]. In some cases, however, ROS may negatively regulate autophagy. The key autophagy-related proteins Atg3 and Atg7 are oxidized by ROS in a thiol-dependent process that prevents LC3 lipidation and autophagosome maturation [10]. The overproduction of ROS by NOX activation

* Corresponding author.
*E-mail address:* lee@snu.ac.kr (B.-H. Lee).

https://doi.org/10.1016/j.redox.2020.101751
Received 26 August 2020; Received in revised form 24 September 2020; Accepted 2 October 2020
Available online 12 October 2020

**Abbreviations**

| | |
|---|---|
| β-actin | actin beta |
| AMPK | AMP-activated protein kinase |
| ATG | autophagy-related |
| BafA1 | bafilomycin A1 |
| ,CM-$H_2$DCFDA | 5- (and-6)-chloromethyl-2′,7′-dichlorodihydrofluorescein diacetate |
| COX | cyclooxygenase |
| CQ | chloroquine |
| DRP1 | dynamin like 1 |
| GFP | green fluorescent protein |
| LAMP1 | lysosomal associated membrane protein 1 |
| MAP1LC3B/LC3B | microtubule-associated protein 1 light chain 3 beta |
| MnSOD | manganese-dependent superoxide dismutase |
| MPH | mouse primary hepatocytes |
| NAC | *N*-acetylcysteine |
| NOX | NADPH oxidase |
| NSAID | nonsteroidal anti-inflammatory drug |
| OCR | oxygen consumption rate |
| ROS | reactive oxygen species |
| ROT | rotenone |
| SQSTM1/p62 | sequestosome 1 |
| TFEB | transcription factor EB |
| TMRE | tetramethylrhodamine ethyl ester |

impairs autophagic flux by decreasing lysosomal acidification and thus lysosomal activity in neuroblastoma cellular models of Parkinson's disease [11–13]. The same is true in the case of oxidative stress-induced cellular premature senescence. ROS induce the dysfunction of mitochondria and then lysosomes, leading to the impairment of autophagic flux crucial for stress-induced premature senescence [14]. Zheng reported that ginsenoside Ro activates NOX and ROS production in esophageal cancer cells. The researchers found that ginsenoside-induced ROS instigate autophagic flux inhibition by impairing autophagosome-lysosome fusion [15]. Therefore, ROS may either activate or inhibit autophagy depending on the cellular microenvironment and conditions of ROS production.

The liver is rich in lysosomes and has a high level of stress-induced autophagy [16]. Autophagy and lysosomal biogenesis are cellular protective mechanisms that occur in response to a variety of stresses. Autophagy plays an important role in maintaining steady-state cellular metabolic processes in the liver, which is critical for the quality and quantity control of organelles and cytosolic proteins in hepatocytes. When the homeostatic regulation of autophagic flux is compromised either chemically or pathophysiologically, hepatic function is affected and occasionally leads to cell death. Acetaminophen overdose induces liver injury, which is the primary cause of acute liver failure. Mitochondrial dysfunction and oxidative stress play a critical role in acetaminophen-induced hepatotoxicity. Acetaminophen induces autophagy, which is a kind of cellular defense machinery, to remove damaged mitochondria and acetaminophen-induced protein adducts [17,18]. The long-term consumption of ethanol causes alcoholic liver disease due to defects in mitochondrial respiration, redox balance and lipid metabolism, leading to hepatic cell death. While acute ethanol treatment in mouse liver and primary hepatocytes activates autophagy to cope with acute cellular adverse events [19,20], chronic alcohol consumption inhibits autophagy flux due to impaired lysosome biogenesis and function [21]. In both cases of chemical-induced liver injury, the pharmacological activation of autophagy protects against hepatotoxicity in part owing to the efficient removal of damaged protein and organelles [17,19].

The molecular mechanisms by which NSAIDs induce hepatic injury have long been studied. However, thus far, little is known about the effects of NSAIDs on autophagy or the exact role and molecular mechanism of autophagy in NSAID-induced hepatotoxicity. In the present study, we intended to clarify the causal relationship between autophagy and NSAID-induced hepatotoxicity. We investigated the effects of autophagy on diclofenac-induced hepatotoxicity. We also analyzed the cellular response following exposure to NSAIDs in terms of autophagic flux. The roles of ROS and lysosomes in the cellular autophagic response were also investigated. Our results provide novel insight into the role of autophagy in NSAID-induced acute hepatotoxicity.

## 2. Results

NSAIDs induce autophagosome accumulation in HepG2 cells and mouse primary hepatocytes (MPH).

We first investigated the effects of diclofenac on autophagy in HepG2 human hepatoma cells and MPH. We identified that diclofenac increased LC3-II, SQSTM1 and NBR1 protein levels in HepG2 cells in a concentration- and time-dependent manner (Fig. 1A). The mRNA levels of *map1lc3b* and *nbr1* were not changed, but the level of *sqstm1* was increased significantly by treatment with diclofenac (Fig. 1B). Due to the autophagy-independent transcriptional upregulation of *sqstm1*, we used NBR1 as a marker of autophagy substrate throughout the experiments. Diclofenac-induced changes in the abundance of proteins associated with autophagy were very similar in MPH (Fig. 1C). Fluorescence microscopy analysis of cells transfected with green fluorescence protein (GFP)-tagged LC3 confirmed that diclofenac increased the number of GFP-LC3 puncta (Fig. 1D). Transmission electron microscopy was used to further investigate the morphological changes induced by diclofenac. Compared to vehicle control, diclofenac treatment induced the accumulation of representative ultrastructural morphological features of autophagosomes, including double-membrane vacuolar structures containing undigested cytoplasmic contents (Fig. 1E). To test whether other NSAIDs showed the same effect on hepatocyte autophagy as diclofenac, we investigated the effects of 6 NSAIDs on autophagy in HepG2 cells. To exclude the possible effect of different cytotoxicity of the drugs on autophagy, we set the highest concentration of all drugs to half of the IC50 determined by an MTT assay. Immunoblot analysis showed that all NSAIDs tested in this study induced a remarkable increase in LC3-II, SQSTM1 and NBR1 levels (Fig. S1). These data demonstrate that NSAIDs with chemical structures closely related to diclofenac induce the accumulation of autophagosomes in HepG2 cells.

### 2.1. Diclofenac inhibits autophagic flux in HepG2 cells and MPH

Based on these findings, we investigated whether diclofenac inhibits autophagic flux, a measure of autophagic degradation activity that enables the differentiation of the nature of the temporal change in the number of autophagosomes. Inhibition of either the fusion of autophagosomes with lysosomes or lysosomal activity impairs overall autophagic degradation. We investigated the effects of diclofenac on autophagic flux using the autophagy inhibitor chloroquine (CQ), a lysosomotropic agent that inhibits autophagosome-lysosome fusion, or bafilomycin A1 (BafA1), a V-ATPase inhibitor that blocks the acidification of lysosomes. Incubation of HepG2 cells with CQ increased the expression of LC3-II and NBR1. However, coincubation with diclofenac failed to further increase the accumulation of the proteins, indicating that diclofenac inhibits autophagic flux (Fig. 2A). To monitor the flux of LC3-II, we transfected the cells with the tandem fluorescence-labelled GFP-mCherry (monomeric red fluorescent protein)-LC3 construct. The

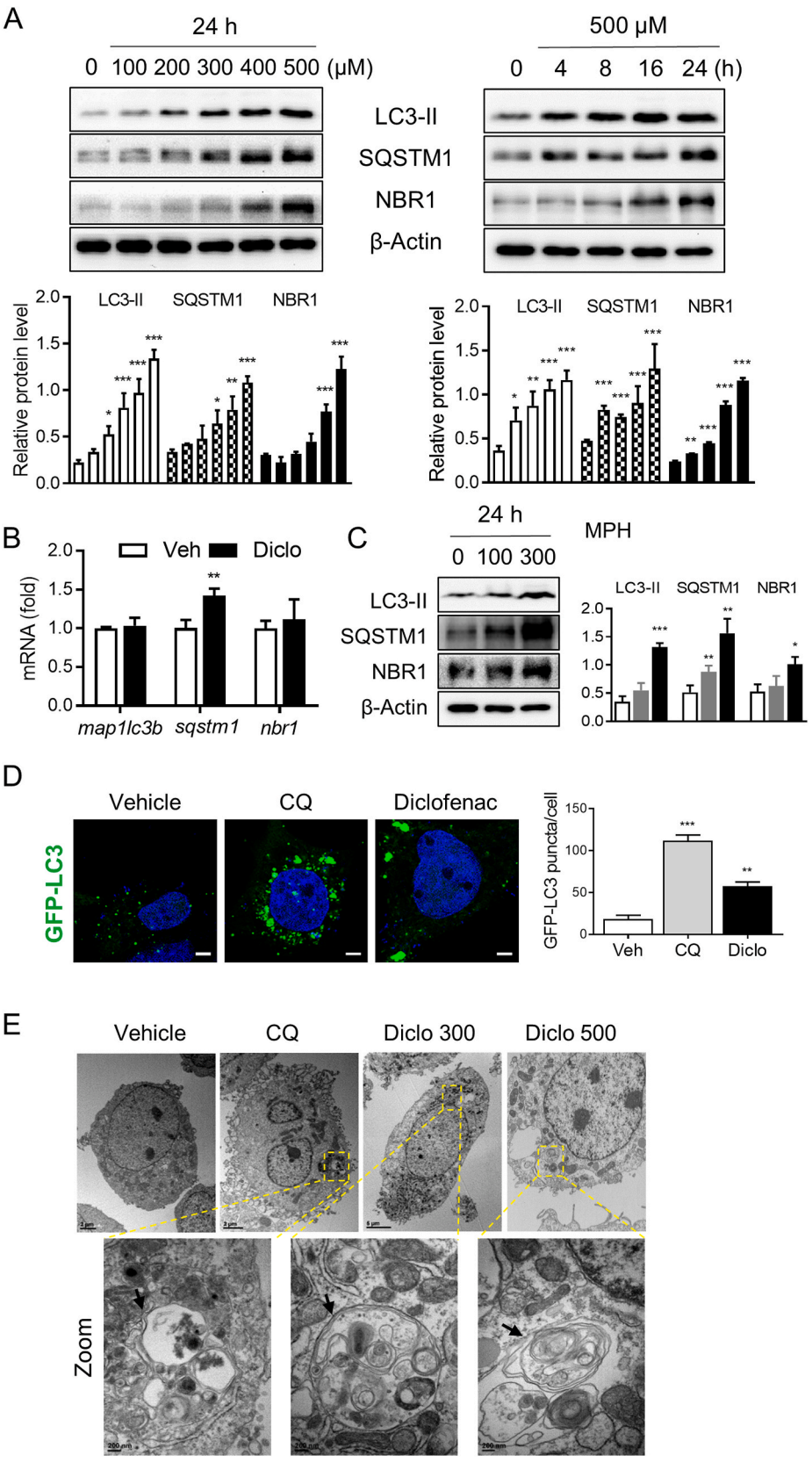


**Fig. 1.** Diclofenac induces autophagosome accumulation in hepatoma cells and mouse primary hepatocytes (MPH). HepG2 cells (A, B) or MPH (C) were treated with diclofenac as indicated and subjected to Western blot analysis with antibodies against LC3-II, SQSTM1 and NBR1 (A, C). Total RNA isolated from the cells treated with diclofenac (500 μM; 24 h) was subjected to qRT-PCR analysis to quantify the relative expression of *mapllc3b, sqstm1*, and *nbr1* (B). (D) HepG2 cells transfected with GFP-LC3 were treated with diclofenac (500 μM; 24 h) or chloroquine (CQ, 50 μM; 4 h). Representative images are shown (scale bar: 4 μm). GFP-LC3 spots were calculated using Image J software. (E) Representative transmission electron microscopy images of the cells treated with diclofenac (300 or 500 μM; 24 h) or CQ (50 μM; 4 h). The enlarged images are magnified from the boxed areas of the upper images. All data are the mean ± SD of at least 3 independent experiments. *$p < 0.05$, **$p < 0.01$, ***$p < 0.001$.

number of both yellow (autophagosome) and red fluorescent puncta (autolysosome) was increased in cells maintained in nutrient-starved Earle's balanced salt solution (EBSS) medium. When the cells were treated with diclofenac, the number of yellow puncta was increased markedly without any significant increase in the number of red puncta. The cells treated with BafA1 also showed a marked increase in the yellow puncta relative to the red puncta (Fig. 2B and C). Similar results were observed in MPH treated with diclofenac (Fig. S5A). The

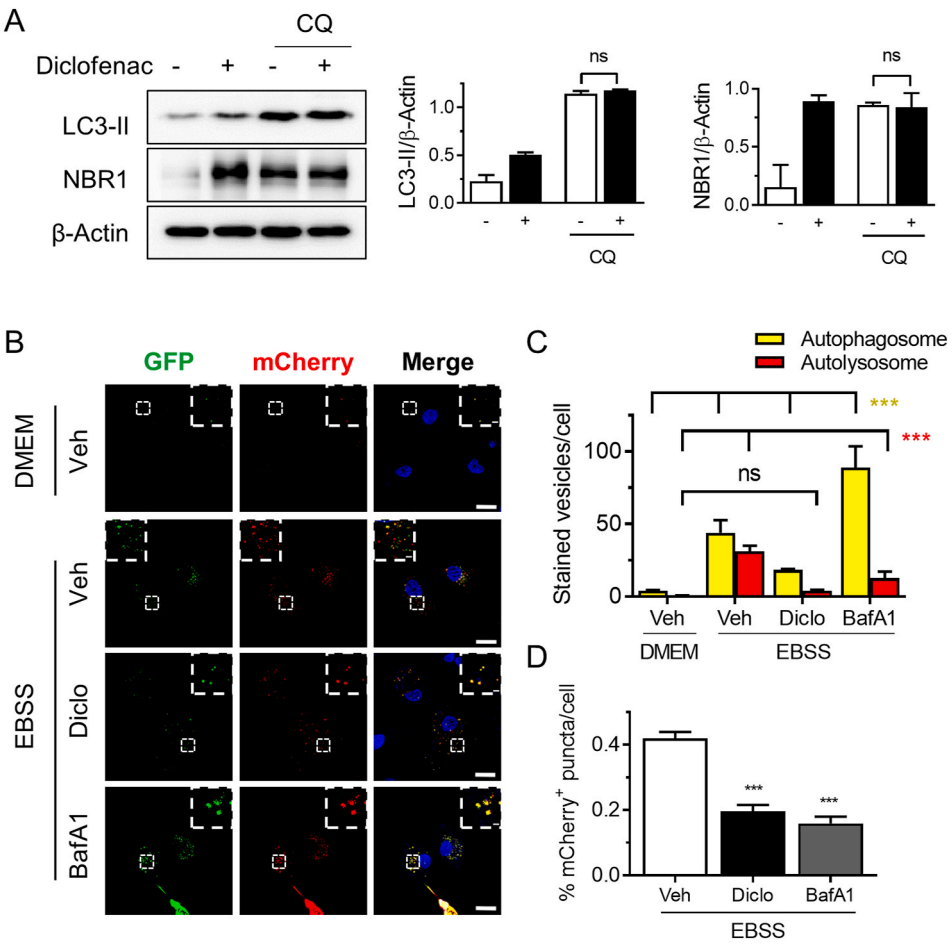


**Fig. 2.** Diclofenac suppresses autophagic flux in human hepatoma cells. (A) HepG2 cells were treated with diclofenac (500 μM; 24 h) in the presence or absence of chloroquine (CQ, 50 μM; 4 h) and subjected to Western blot analysis with antibodies against LC3-II and NBR1. Representative Western blot images and the relative quantification of the protein are shown. (B) HepG2 cells transfected with GFP-mCherry-LC3 were incubated under starved conditions and treated with diclofenac (500 μM; 24 h) or BafA1 (100 nM; 8 h). Representative fluorescent images of the cells are shown. The zoomed images in the upper right or left corners were magnified from the small boxed areas in each image (scale bars: 20 μm; magnification, 2 μm). (C) Quantification of autophagosomes (yellow dots) and autolysosomes (red dots) in cells transfected with GFP-mCherry-LC3 and (D) the percentage of mCherry puncta exhibiting autolysosomes per cell were analyzed. All data are the mean ± SD of at least 3 independent experiments. ***$p < 0.001$ and ns, not significant. (For interpretation of the references to color in this figure legend, the reader is referred to the Web version of this article.)

percentage of mCherry$^+$ puncta relative to the total puncta per cell in merged images was calculated. The number of mCherry$^+$ puncta (autolysosomes) per total puncta (autophagosomes and autolysosomes) was significantly lower in diclofenac- or BafA1-treated cells than in cells maintained in EBSS. The vehicle-treated cells were not included in the analysis due to very low numbers of stained vesicles per cell (Fig. 2D). The inhibition of autophagy by other NSAIDs shown in Fig. S1 was also confirmed using GFP-mCherry-LC3-transfected cells (data not shown). Next, we questioned whether cyclooxygenase (COX) inhibitory activity has to do with the effect of NSAIDs on autophagy. To this end, we compared the effects of (*S*)- and (*R*)-ibuprofen with and without COX inhibitory activity, respectively, on autophagy in HepG2 cells. We found that both stereoisomers inhibited autophagy flux to a similar degree (Fig. 3A and B). Moreover, no change in autophagy marker proteins was observed when knocking down *Cox1* in MPH or treating MPH with aspirin, a representative COX1/2 inhibitor (Fig. S2). Taken together, these results suggest that the COX inhibitory activity is not a critical factor determining the effects of diclofenac on autophagy.

The increase in the number of GFP-LC3 puncta and in the yellow fluorescence of GFP-mCherry-LC3-transfected cells and the results of Western blot analysis that showed increased LC3-II and NBR1 protein levels suggest that NSAIDs may inhibit the late stage of autophagy. To confirm this hypothesis, we checked whether diclofenac affects the biogenesis of a preautophagosomal double-membrane structure that originates from the omegasome. We analyzed the distribution of the omegasome markers WDFY-mCherry and GFP-LC3 in cells treated with diclofenac. In line with the Western blot data in Fig. 1A, the number of LC3 spots was increased by treatment with diclofenac. However, diclofenac did not change the number of WDFY spots. We did not observe the colocalization of LC3 with WDFY, which was evident in the cells cultured in EBSS (Fig. S3). Finally, we investigated whether diclofenac impairs autophagic flux in cells with activated basal autophagy. While rapamycin treatment increased the number of autolysosomes, a marked increase in the number of autophagosomes was observed under diclofenac treatment in the presence of rapamycin (Fig. S4A). The results clearly indicate that GFP quenching in lysosomes was impaired in cells treated with diclofenac. Taken together, these data demonstrate that diclofenac impairs basal and stimulated autophagic flux at the late stage.

### 2.2. *Diclofenac inhibits lysosomal activity and fusion with autophagosomes*

Autophagic flux may become inhibited when lysosomal hydrolase activity decreases due to an increase in lysosomal pH or when the fusion of autophagosomes with lysosomes is inhibited. Therefore, we analyzed cathepsin B activity in cells treated with diclofenac or cathepsin B inhibitor as a control. Diclofenac significantly lowered the enzyme activity (Fig. 4A). To further investigate the effects of diclofenac on lysosomal activity, we used Cathepsin Magic Red, which is cleaved in the presence of active cathepsins to produce a fluorescent product. Diclofenac substantially reduced the fluorescence intensity, supporting the result of the lowered cathepsin B activity. (Fig. 4B). Next, we measured lysosomal pH using DQ-BSA red, a self-quenching fluorescent probe that does not undergo proteolysis in the acidic environment of lysosomes, or LysoSensor Green, a pH-sensitive dye that becomes more fluorescent in acidic organelles. Incubation of the cells with diclofenac led to a strong reduction in DQ-BSA red and LysoSensor Green fluorescence, indicating elevated lysosomal pH and thus impaired lysosomal activity (Fig. 4C). To address whether the inhibition of autophagic flux by diclofenac resulted from the failure of lysosomes to fuse with autophagosomes, we

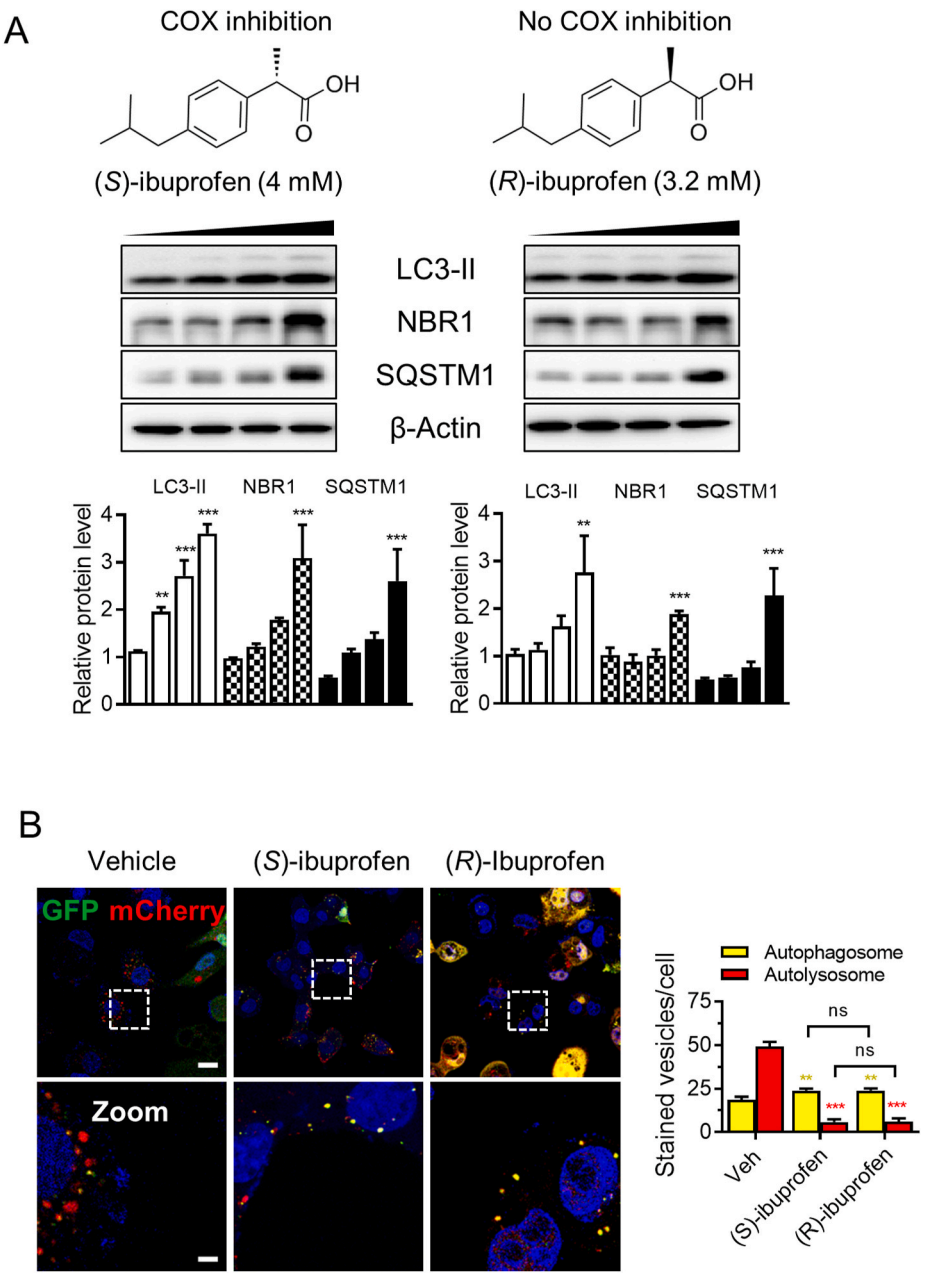


**Fig. 3.** Autophagy impairment by NSAIDs is independent of COX inhibition. (A) Chemical structures of (*S*)- and (*R*)-ibuprofen. HepG2 cells were incubated with (*S*)-ibuprofen (1, 2, 4 mM) or (*R*)-ibuprofen (0.8, 1.6, 3.2 mM) for 24 h. The protein levels of LC3-II, NBR1 and SQSTM1 were measured by Western blot analysis. Representative Western blot images and the relative quantification of proteins are shown. (B) HepG2 cells expressing GFP-mCherry-LC3 were incubated for 24 h with (*S*)-ibuprofen (4 mM) or (*R*)-ibuprofen (3.2 mM). Representative fluorescent images of the cells are shown. The zoom images were magnified from the boxed areas in each image (scale bars: 20 μm; magnification, 4 μm). Quantitative data represent the number of autophagosomes (yellow dots) and autolysosomes (red dots) in cells transfected with GFP-mCherry-LC3 (n > 20 cells per experiment). All data are the mean ± SD of at least 3 independent experiments. $^{**}p < 0.01$, $^{***}p < 0.001$ *and ns, not significant.* (For interpretation of the references to color in this figure legend, the reader is referred to the Web version of this article.)

transfected cells with GFP-LC3 and examined the colocalization of LC3 with lysosome-associated membrane protein 1 (LAMP1), a marker of lysosomes and late endosomes, in the absence or presence of diclofenac. BafA1 was used as an inhibitor of autophagic flux that blocks the acidification of lysosomes. The GFP-LC3 puncta accumulated in the presence of BafA1 were distinctly surrounded by the lysosomal membrane that is visualized by LAMP1 antibody. In contrast, we were not able to observe the colocalization of GFP-LC3 and LAMP1 in cells treated with diclofenac, suggesting the inhibition of fusion between autophagosomes and lysosomes. The quantification of the puncta clearly shows that diclofenac significantly reduced the ratio of the number of GFP-LC3 puncta in lysosomes to total GFP-LC3 puncta (Fig. 4D).

We investigated whether the reactivation of lysosomal function restores the autophagic activity that is suppressed by diclofenac. For this, we used clioquinol, which induces lysosomal acidification and thus hydrolase activity, as a membrane-permeable zinc ionophore [22]. We also used cells transfected with a plasmid containing transcription factor EB (*p*-ENTR-CMV-TFEB), a master transcription factor of lysosomal biogenesis and autophagy. The diclofenac-induced accumulation of the proteins LC3-II and NBR1 was relieved by clioquinol or TFEB (Fig. 5A). Clioquinol reversed the diclofenac-induced failure in autolysosome formation, as evidenced by the increased number of red fluorescence puncta in cells transfected with the GFP-mCherry-LC3 construct (Fig. 5B). The determination of lysosomal pH using LysoSensor Green revealed that clioquinol treatment markedly increased the fluorescence intensity, implying the reacidification of lysosomes (Fig. 5C). Reactivation of autophagic flux and reacidification of lysosomes by clioquinol were also observed in MPH (Figs. S5A and B). Taken together, our results indicate that diclofenac inhibits autophagic flux by suppressing the fusion of lysosomes with autophagosomes and by inducing an increase in lysosomal pH and thus decreasing lysosomal activity.

Diclofenac-induced ROS are responsible for the impairment of lysosomal activity and autophagy.

We explored the mechanism by which diclofenac inhibits autophagic flux in hepatocytes. Diclofenac is known to produce superoxide by inhibiting mitochondrial oxidative phosphorylation or by activating

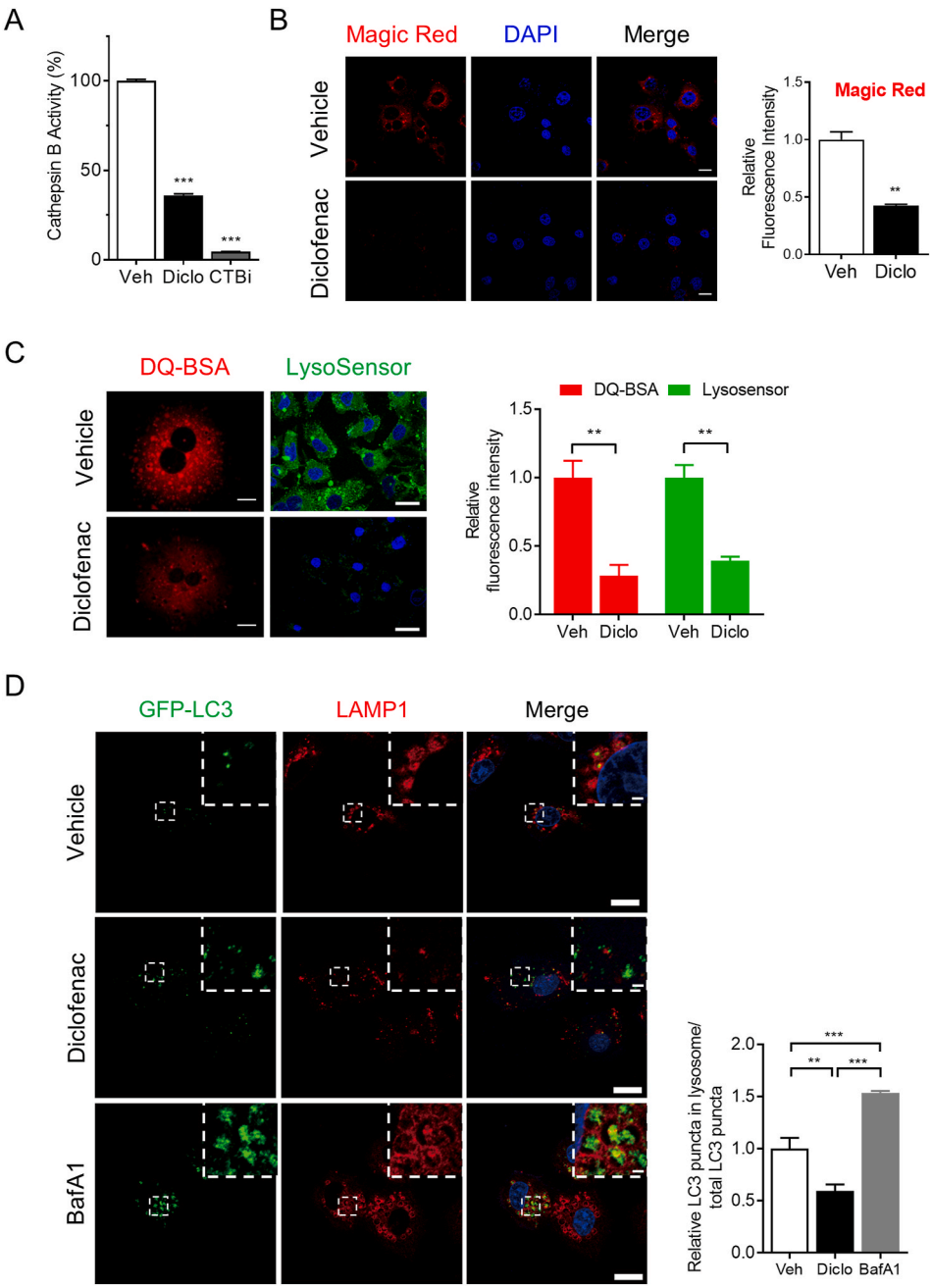


**Fig. 4.** Diclofenac inhibits lysosomal activity and fusion with autophagosomes. (A) HepG2 cells were treated with diclofenac or Cathepsin B inhibitor (CTBi) for 24 h. Cathepsin B activity was measured using a cathepsin B activity fluorometric kit. (B, C) The cells were treated with diclofenac (500 μM; 24 h), and the lysosomal activity and acidity were analyzed by Magic Red (B), DQ-BSA Red and LysoSensor Green DND-189 (scale bars: 20 μm) (C), respectively. Nuclei were stained with DAPI (blue). The fluorescence intensity is calculated using Image J software. (D) HepG2 cells expressing GFP-LC3 (green) were incubated with diclofenac (500 μM; 24 h) or bafilomycin A1 (BafA1, 100 nM; 8 h). The fixed cells were subjected to immunofluorescence analysis with antibodies against LAMP1 (red). Nuclei were stained with DAPI (blue). Representative confocal microscopy images are shown. The zoomed images in the upper right corners were magnified from the small boxed areas in each image (scale bars: 20 μm; magnification, 2 μm). The relative number of GFP-LC3 spots in lysosomes versus that of total GFP-LC3 spots was plotted. All data are the mean ± SD of at least 3 independent experiments. $^{**}p < 0.01$, $^{***}p < 0.001$. (For interpretation of the references to color in this figure legend, the reader is referred to the Web version of this article.)

NOX depending on the target tissue [5,23]. Evidence suggests that ROS modulate autophagy differently depending on the cellular environment. ROS activate autophagy as a survival mechanism to minimize cellular damage. However, the oxidative stress induced as a result of mitochondrial or lysosomal dysfunction impairs autophagy, which is observed in the cellular model of aging and senescence [14]. We determined general oxidant, mitochondrial and cytosolic superoxide and mitochondrial $H_2O_2$ levels by measuring the relative fluorescence of CM-$H_2$DCFDA, MitoSOX, dihydroethidium and Mito-PY1, respectively. Diclofenac increased the intracellular levels of ROS, mitochondrial and cytosolic superoxide and mitochondrial $H_2O_2$ in a dose-dependent manner (Fig. 6A). We also found that the NSAIDs tested in this study increased cellular ROS levels within the concentrations that inhibited autophagy (Fig. S6). Moreover, the diclofenac-induced impairment of lysosomal activity and autophagy were completely restored by pretreatment with the antioxidant *N*-acetylcysteine (NAC) or Mito-Tempo, a mitochondria-targeted superoxide scavenger. The increase in the intensity of LysoSensor Green fluorescence indicates that the lysosomal pH was brought back into the acidic range (Fig. 6B). As a result, the protein levels of LC3-II and NBR1 were decreased, and the autophagic flux was recovered by NAC and Mito-Tempo, as evidenced by the increased number of red fluorescence puncta in GFP-mCherry-LC3-transfected cells (Fig. 6C and D). The reactivation of autophagic flux by NAC was also observed in MPH (Fig. S7). As explained earlier in Fig. S4A, autophagic flux was not recovered when diclofenac and rapamycin were treated simultaneously. Neither the level of ROS nor the lysosomal activity was affected under the experimental conditions (Figs. S4B and C). Finally, transfection of the cells with manganese superoxide dismutase (MnSOD) decreased the level of mitochondrial superoxide significantly, which reversed the effects of diclofenac on the lysosomal function and autophagy (Fig. S8). These data clearly show that the mitochondrial ROS produced by diclofenac are responsible for the impairment of lysosomal

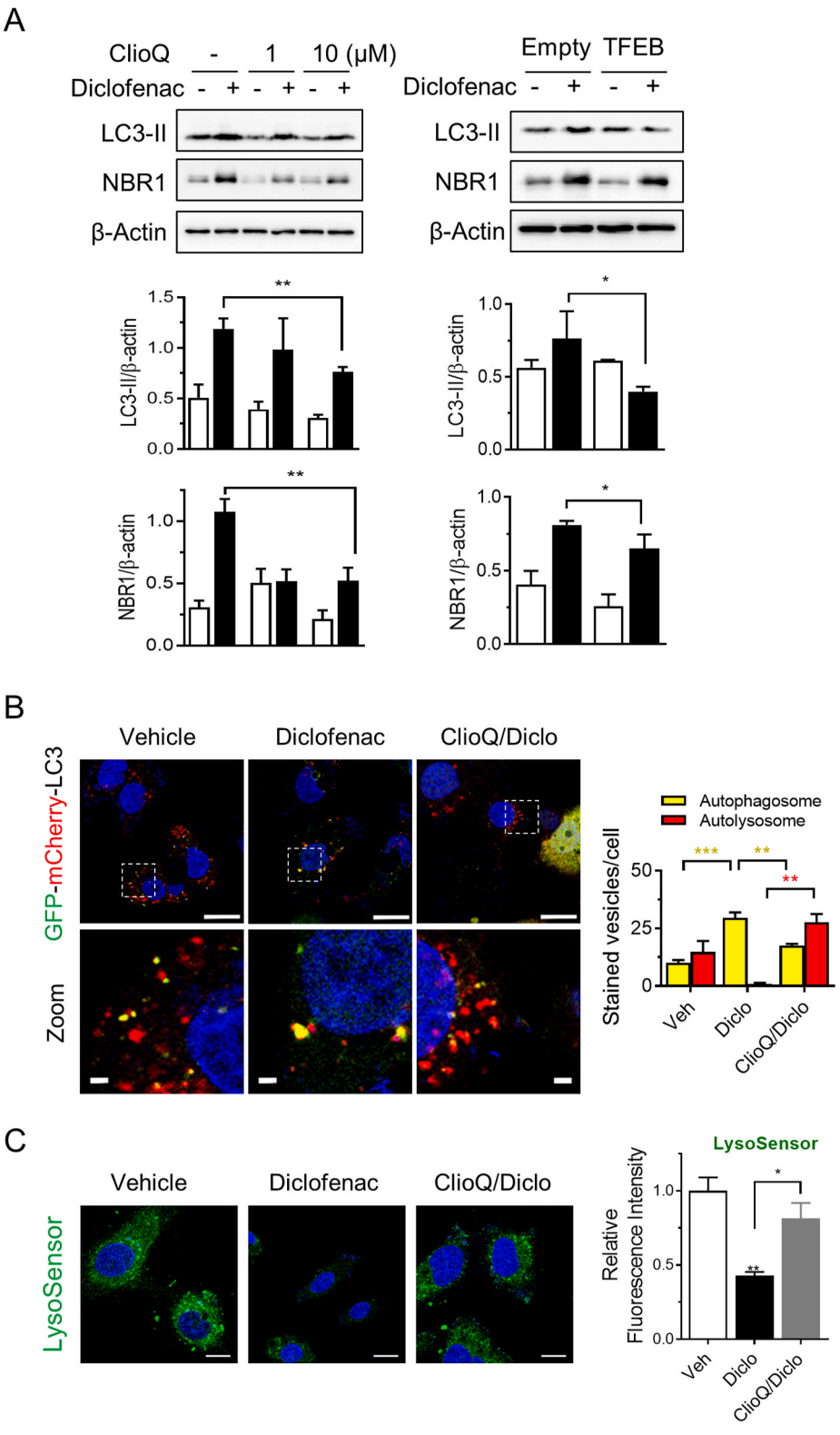


**Fig. 5.** Lysosomal reactivation restores diclofenac-induced autophagy impairment. (A) HepG2 cells pretreated with clioquinol (ClioQ, 10 μM) for 1 h or transfected with pENTR-CMV-TFEB or empty control vector were exposed to diclofenac (500 μM; 24 h) and subjected to Western blot analysis with antibodies against LC3-II and NBR1. Representative Western blot images and the relative quantification of protein expression are shown. (B) The cells transfected with GFP-mCherry-LC3 were treated with diclofenac for 24 h in the absence or presence of ClioQ (10 μM). The zoomed images are magnified from the boxed areas in the overlay images (scale bars: 20 μm; magnification, 2 μm). Quantification of autophagosomes (yellow dots) and autolysosomes (red dots) in cells transfected with GFP-mCherry-LC3 was analyzed. (C) Lysosomal acidity was analyzed by LysoSensor Green DND-189 (scale bar: 10 μm). Representative fluorescent images of the cells are shown. The fluorescence intensity is calculated using Image J software. All data are the mean ± SD of at least 3 independent experiments. *p < 0.05, **p < 0.01, ***p < 0.001. (For interpretation of the references to color in this figure legend, the reader is referred to the Web version of this article.)

activity and autophagy.

Next, we investigated whether NOX-derived ROS contribute to the suppression of autophagy. Isoforms of NOX enzymes have been identified in various cells and tissues. NOX3 and NOX4 are the predominant forms expressed in the liver, while HepG2 cells exclusively express NOX3 [24,25]. PCR analysis revealed that diclofenac increased the expression of *Nox3* in HepG2 cells (Fig. S9A). However, the knockdown of the *Nox3* gene or pretreatment with ML171, a specific NOX3 inhibitor, marginally alleviated diclofenac-induced autophagy inhibition, if at all (Fig. S9B). The ROS produced by xanthine oxidase [26] were also not responsible for the autophagy inhibition induced by diclofenac (Fig. S9C). From these data, we can conclude that mitochondria are the major source of ROS, while NOX partially contributes to the diclofenac-mediated impairment of autophagy.

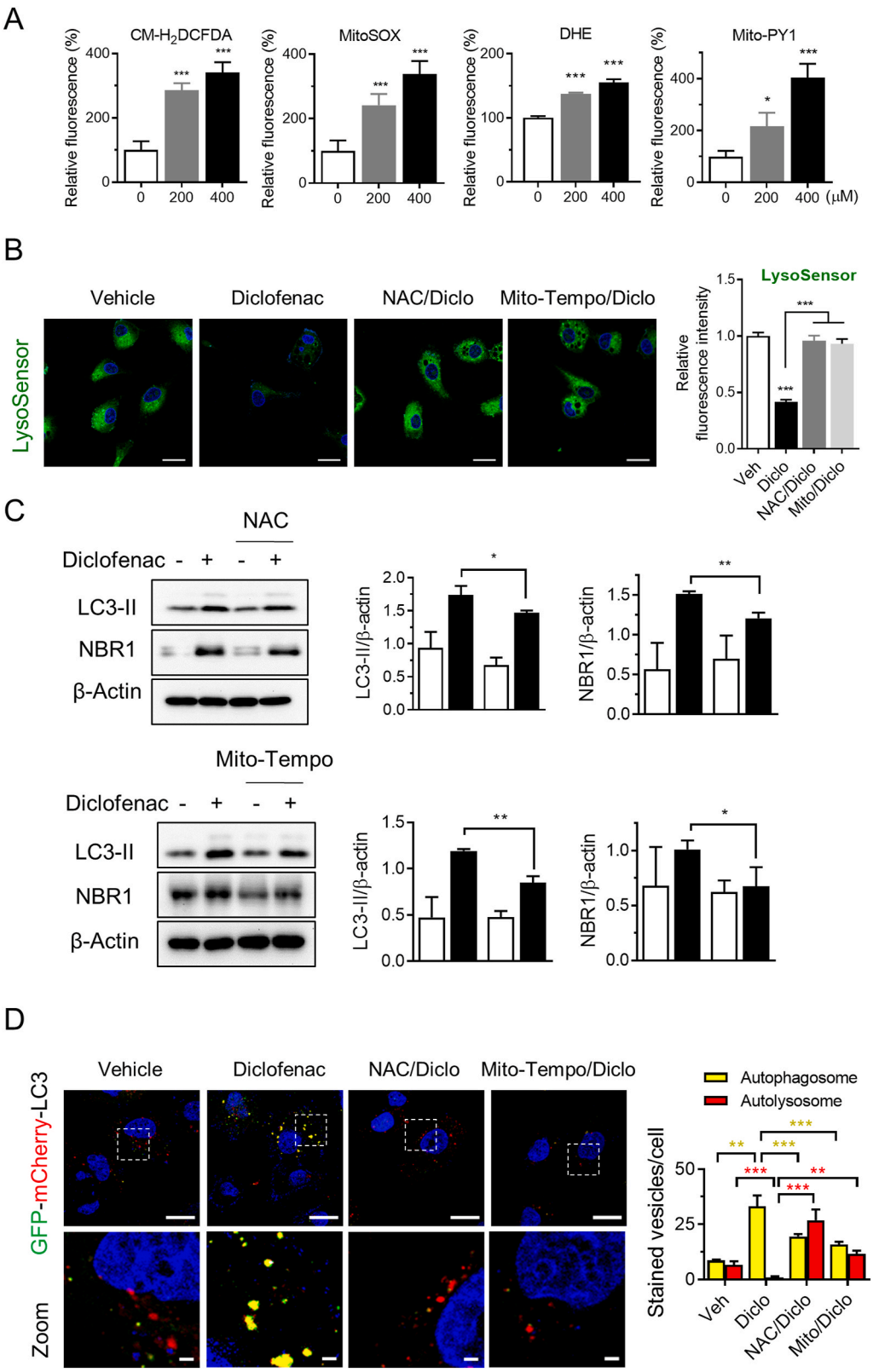


**Fig. 6.** Diclofenac-induced ROS are responsible for the impairment of lysosomal activity and autophagy. (A) HepG2 cells were treated with diclofenac for 16 h at the indicated concentrations, and the cellular and mitochondrial ROS levels were measured by quantifying the fluorescence of CM-$H_2$DCFDA, dihydroethidium, MitoSOX and Mito-PY1 using flow cytometry. (B–D) The cells were pretreated with *N*-acetylcysteine (NAC; 2 mM) or Mito-Tempo (20 μM) for 1 h, and further incubated with diclofenac (500 μM; 24 h). The cells were stained with LysoSensor Green DND-189 (scale bar: 20 μm) (B) or subjected to Western blot analysis with antibodies against LC3-II and NBR1. Representative Western blot images and the relative quantification of proteins are shown (C). HepG2 cells expressing GFP-mCherry-LC3 were incubated as described in (B) and were analyzed by confocal microscopy. The zoomed images are magnified from the boxed areas in the overlay images (scale bars: 20 μm; magnification, 2 μm). Representative images are shown and quantitative data represent the number of autophagosomes (yellow dots) and autolysosomes (red dots) in cells transfected with GFP-mCherry-LC3 (n > 20 cells per experiment) (D). All data are the mean ± SD of at least 3 independent experiments. *p < 0.05, **p < 0.01, ***p < 0.001. (For interpretation of the references to color in this figure legend, the reader is referred to the Web version of this article.)

### 2.3. Diclofenac induces mitochondrial oxidative stress and dysfunction

Studies suggest that mitochondrial dysfunction and ROS production play an important role in diclofenac-induced hepatotoxicity [4]. To correlate the production of ROS and mitochondrial function, we first analyzed mitochondrial DNA damage by quantitative RT-PCR of cytochrome *c* oxidase subunit I. Diclofenac downregulated the expression of this mRNA in a dose-dependent manner (Fig. 7A). The oxidative modification of mitochondrial proteins and lipids was also monitored. The oxidation levels of ROS-sensitive mitochondrial proteins were measured by the alkylation of the low pKa cysteine residue using biotinylated iodoacetamide. The oxidation of the mitochondrial lipid

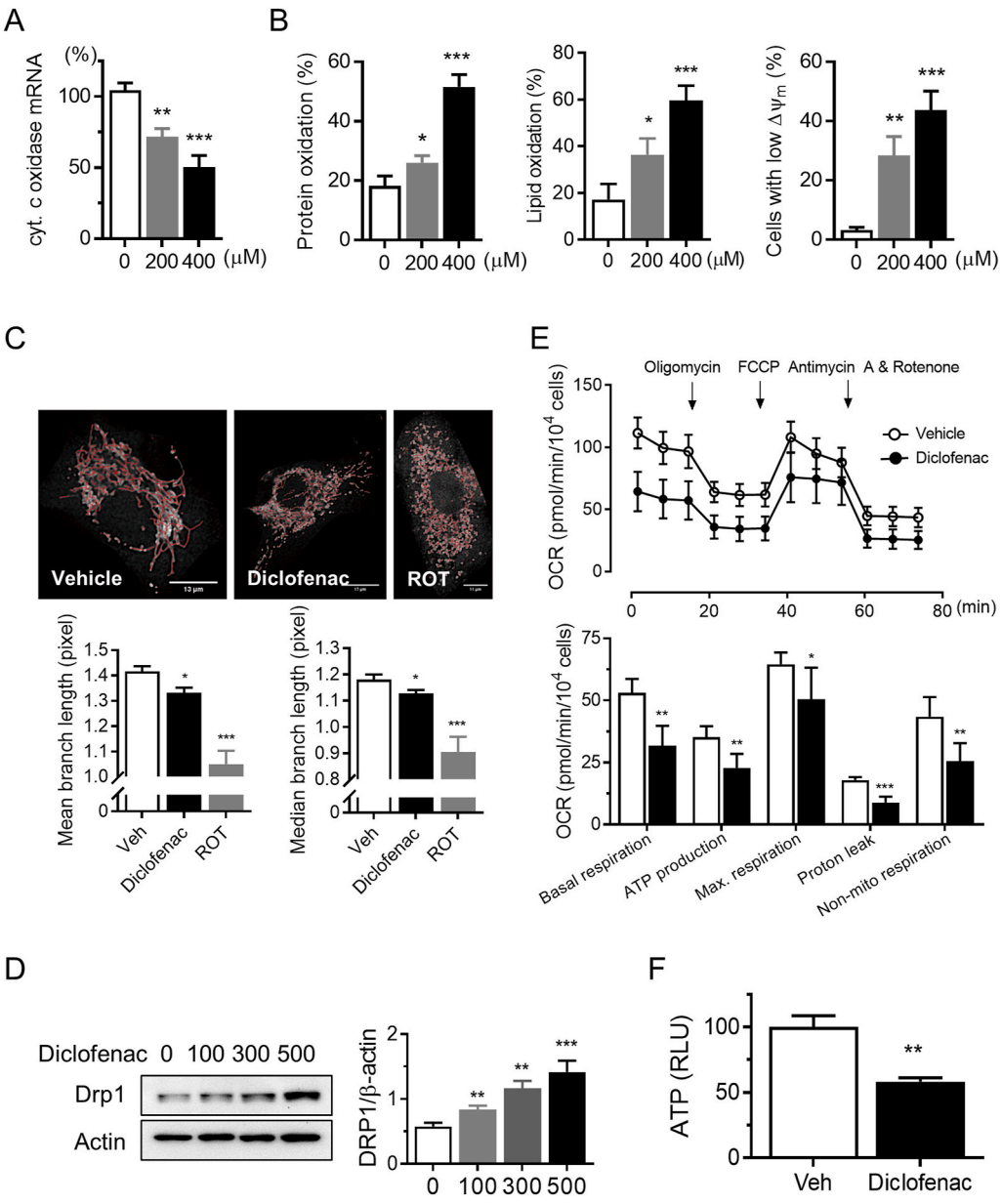


**Fig. 7.** Diclofenac induces oxidative mitochondrial damage and mitochondrial dysfunction in human hepatoma cells. (A, B) HepG2 cells were cultured with diclofenac for 16 h. (A) Total RNA was isolated and subjected to qRT-PCR analysis to measure cytochrome *c* oxidase mRNA expression. (B) The oxidation levels of ROS-sensitive mitochondrial proteins were measured by blot analysis using HRP-conjugated streptavidin. Oxidation of mitochondrial lipid cardiolipin and mitochondrial membrane potential were analyzed by flow cytometry following staining with nonyl acridine orange and tetramethylrhodamine ethyl ester (TMRE), respectively. (C) The cells were incubated with diclofenac (500 μM) or rotenone (ROT, 100 μM) for 8 h, and the mitochondria were stained with MitoTracker Red. Images were obtained by confocal microscopy and analyzed with ImageJ with the Mitochondrial Network Analysis (MiNA) program. Red lines indicate mitochondrial networks. Mitochondrial networks were analyzed using the mean branch length and median branch length supplied by the MiNA program. (D) The level of fission protein DRP1 was measured by Western blot analysis in the cells treated with diclofenac. (E) Mitochondrial function was analyzed by measuring OCR using a Seahorse XF Cell Mito Stress Test Kit. Each indicator was determined by the Seahorse XF Cell Mito Stress Test Report Generator. (F) ATP levels were measured using the CellTiter-Glo assay. All data are the mean ± SD of at least 3 independent experiments. $^{*}p < 0.05$, $^{**}p < 0.01$, $^{***}p < 0.001$. (For interpretation of the references to color in this figure legend, the reader is referred to the Web version of this article.)

cardiolipin was analyzed using nonyl acridine orange. Diclofenac increased the level of mitochondrial protein and lipid oxidation in a dose-dependent manner. The number of cells with low mitochondrial membrane potential, as measured by the potential-sensitive probe TMRE, was also increased by diclofenac (Fig. 7B). To ascertain mitochondrial dysfunction in response to diclofenac treatment, we evaluated the morphology and function of mitochondria. Cells treated with diclofenac were stained with MitoTracker Red, and confocal microscopy images were analyzed with ImageJ with the Mitochondrial Network Analysis (MiNA) toolset [27]. Rotenone was used as a positive control. Out of the 9 parameters tested, the mean and median rod/branch lengths were significantly reduced by rotenone and by diclofenac (Fig. 7C). The expression of the fission protein DRP1 was increased by diclofenac in a dose-dependent manner (Fig. 7D). These results indicate that longer rods were fragmented into smaller ones and that a few larger networks were broken up into smaller networks by diclofenac. To understand the effects of diclofenac on mitochondrial function, we assessed the respiratory profile using a Seahorse Flux Analyzer. Changes in oxygen consumption rate (OCR) were recorded, and areas under the curve were calculated before and after each treatment with inhibitors of mitochondrial oxidative phosphorylation. We observed a significant decline in mitochondrial respiration in cells treated with diclofenac. Compared to vehicle treatment, diclofenac treatment decreased the mitochondrial OCR at every phase measured (Fig. 7E). Consistent with this result, ATP content was also decreased in cells treated with diclofenac (Fig. 7F). Similar results were obtained in MPH (Fig. S10). Together, our results support that diclofenac induces oxidative mitochondrial damage and mitochondrial fragmentation and dysfunction in hepatocytes.

### 2.4. *Diclofenac inhibits lysosomal colocalization with mitochondria and mitophagy*

The degradation of damaged mitochondria through mitophagy is a key cellular event for proper mitochondrial quality control and function in drug-induced liver injury [18]. To determine whether diclofenac-induced ROS production and lysosomal impairment affect mitophagy, electron microscopy analysis was performed to visualize mitochondrial morphology. Fig. 8A shows the accumulation of

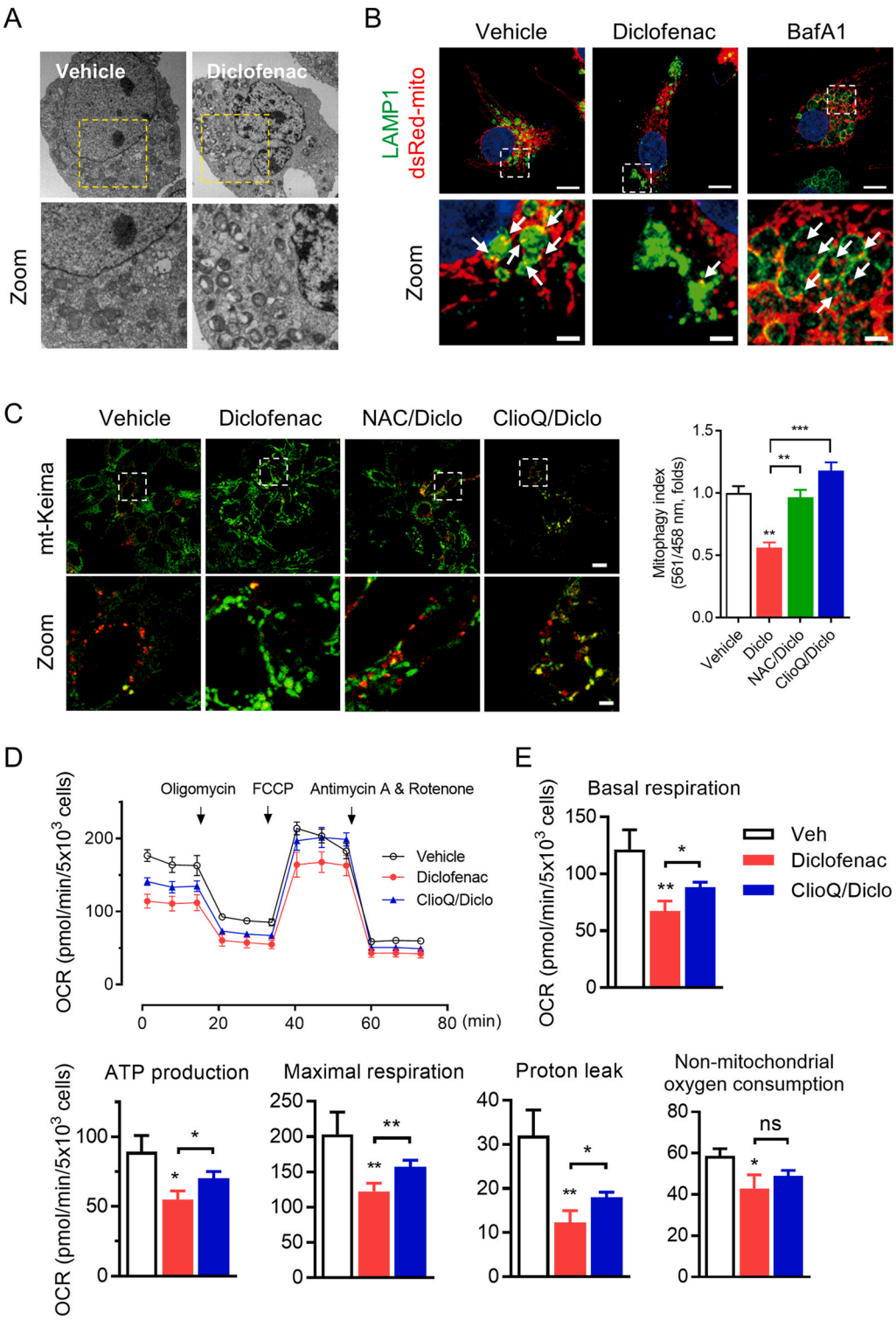


**Fig. 8.** Diclofenac inhibits lysosomal colocalization with mitochondria and mitophagy in hepatocytes. (A) Representative images of mitochondria in HepG2 cells treated with diclofenac were analyzed by transmission electron microscopy. The zoomed images are magnified from the boxed areas of the images. (B) HepG2 cells expressing dsRed-mito (red, mitochondria) were incubated with diclofenac (500 μM) or BafA1 (100 nM) for 8 h under starved conditions. The fixed cells were subjected to immunofluorescence analysis with antibodies against LAMP1 (green). Nuclei were stained with DAPI (blue). Representative confocal microscopy images are shown, with the zoomed images magnified from the boxed areas in the overlay images. White arrows indicate mitochondria in lysosomes (scale bars: 10 μm; magnification, 2 μm). (C) Hep3B cells stably expressing mt-Keima were pretreated with *N*-acetylcysteine (NAC, 2 mM) or clioquinol (ClioQ, 10 μM) for 1 h and then exposed to diclofenac for 8 h. Confocal microscopy was analyzed to detect the mt-Keima located in mitochondria (mitochondria at neutral pH, green) and the mt-Keima puncta delivered to lysosomes (mitochondria at acidic pH, red). The zoom images were magnified from boxed areas in overlay images (scale bars: 20 μm; magnification, 2 μm). Mitophagy index was evaluated by analyzing the ratio of 561/458 nm. (D, E) HepG2 cells pretreated with ClioQ (10 μM) for 1 h were incubated with diclofenac (500 μM) for 24 h. Mitochondrial function was analyzed by measuring oxygen consumption rate (OCR) using the Seahorse XF Cell Mito Stress Test Kit (D). Each indicator was determined by the Seahorse XF Cell Mito Stress Test Report Generator (E). All data are the mean ± SD of at least 3 independent experiments. $*p < 0.05$, $**p < 0.01$. $***p < 0.001$ and ns, not significant. (For interpretation of the references to color in this figure legend, the reader is referred to the Web version of this article.)

abnormal mitochondria with vacuolization and fragmented cristae in cells treated with diclofenac. To determine whether damaged mitochondria are retained within lysosomal organelles, we expressed dsRed-mito to fluorescently label mitochondria, and immunofluorescence analysis was conducted with a LAMP1 antibody. In control cells, a significant number of colocalizations between mitochondria and lysosomes was observed. In cells treated with BafA1, we found enlarged lysosomes that colocalized with mitochondria. In contrast, there was little colocalization in cells treated with diclofenac, indicating the inhibition of the fusion of mitochondria with lysosomes (Fig. 8B). To provide additional evidence for the effects of diclofenac on mitophagy activity, we monitored mt-Keima, a ratiometric pH-sensitive fluorescent protein that is targeted into the mitochondrial matrix. A low-ratio mt-Keima-derived fluorescence represents a neutral environment, whereas a high-ratio fluorescence represents an acidic pH. Thus, mt-Keima enables differential imaging of mitochondria in the cytoplasm and those in acidic lysosomes [28]. To monitor the inhibition of mitophagy, we used Hep3B cells stably transfected with the mt-Keima

construct where the basal level of mitophagy is relatively high [29]. High levels of acidic mitochondria were found in vehicle-treated control cells. However, treatment of the cells with autophagic flux inhibitors, BafA1 or CQ, abated the number of acidic mitochondria (Fig. S11). The cells treated with diclofenac also showed decrease in the red puncta (acidic mitochondria) and treatment with NAC or clioquinol in the presence of diclofenac restored the number of acidic mitochondria (Fig. 8C). As a result, clioquinol improved the mitochondrial function that was suppressed by diclofenac (Fig. 8D and E). These data indicate that diclofenac-induced ROS production and lysosomal impairment inhibit the fusion of the autophagosome containing engulfed mitochondria with lysosomes and thus mitophagy, resulting in the impaired degradation of damaged mitochondria.

### 2.5. Rapamycin inhibits diclofenac-induced cell death and liver injury

Given that autophagy protects against liver injury induced by diverse chemicals, we investigated whether the activation of autophagy by rapamycin modulates diclofenac-induced cytotoxicity and hepatotoxicity. We pretreated HepG2 cells with or without rapamycin, further incubated with diclofenac and monitored cell growth and apoptotic cell death. Diclofenac lowered cell proliferation and increased apoptotic cell death, which were reversed by pretreatment with rapamycin (Fig. 9A and B). Rapamycin reduced the protein levels of LC3-II, NBR1 and SQSTM1 that have been observed to be increased by diclofenac (Fig. 9C). The viability of HepG2 cells exposed with diclofenac concomitant with clioquinol was increased, but cotreatment with CQ

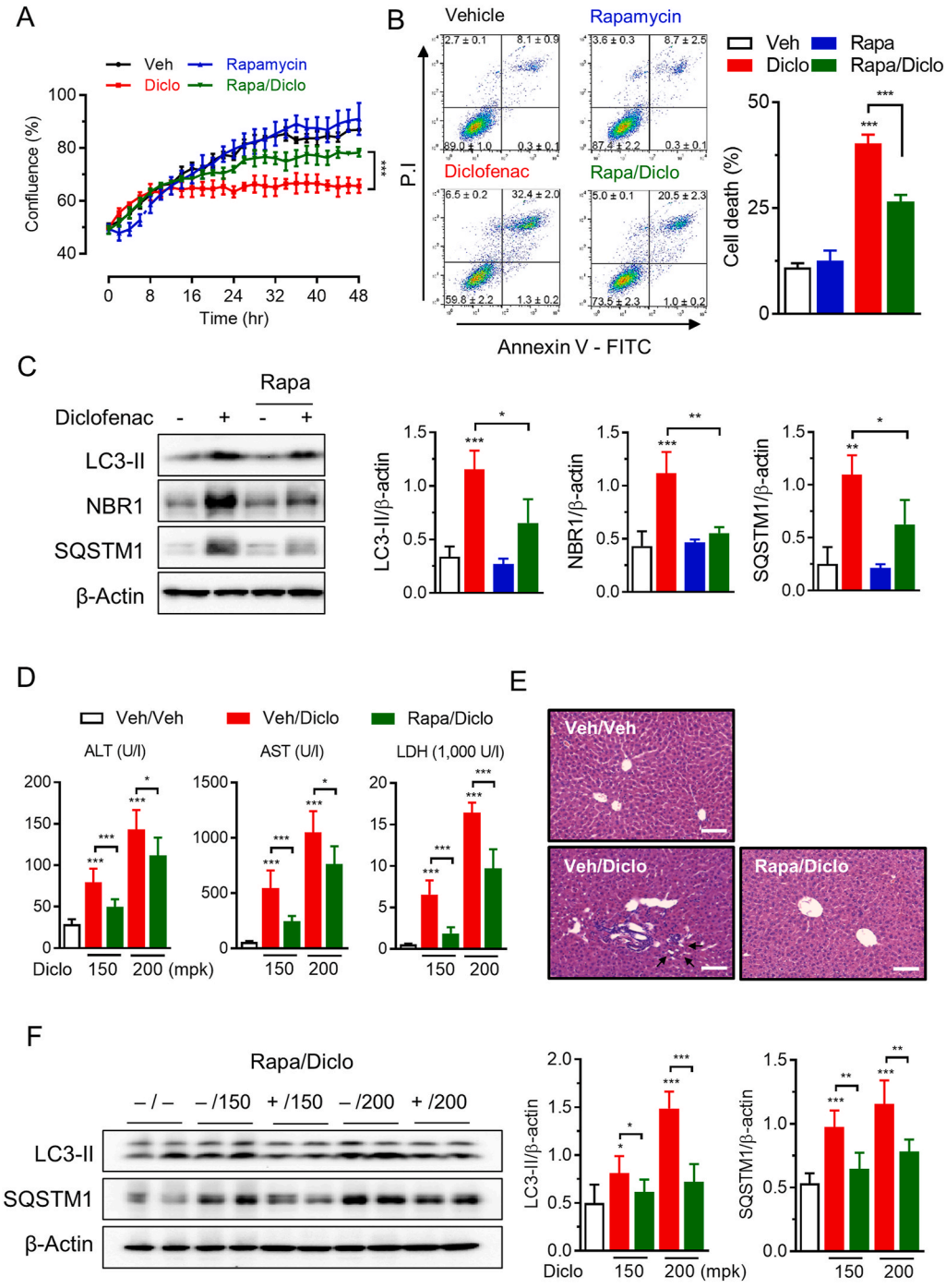


**Fig. 9.** Rapamycin inhibits diclofenac-induced cell death and liver injury in vitro and in vivo. (A) HepG2 cells were pretreated with or without rapamycin (500 nM) for 24 h, and then incubated with diclofenac (500 μM) for 48 h. Cell confluency was determined using a Cytation 3 cell imaging microplate reader. (B) After culture in the absence or presence of rapamycin (500 nM) for 48 h, the cells were further incubated with diclofenac (500 μM) for 16 h and subjected to FACS analysis (left panel). The percentage of cell death was plotted as the sum of the percentage of Annexin-positive, PI-positive and Annexin/PI-positive cells (right panel). (C) HepG2 cells were pretreated with or without rapamycin (500 nM) for 24 h and further incubated with diclofenac (500 μM) for 24 h. Expression of the proteins was analyzed by Western blot analysis using antibodies against LC3-II, NBR1, and SQSTM1 in HepG2 cells incubated as indicated. (D–F) Male C57BL/6 mice were injected intraperitoneally with rapamycin 0.5 h before diclofenac administration and sacrificed after 6 h. (D) Serum ALT, AST and LDH measurements were performed using an automated Chemistry Analyzer (Tokyo Boeki Medical system, Prestige 24I). (E) Liver histology was analyzed using H&E staining. Original magnification, 10X. Arrows indicate the region of sinusoidal telangiectasia (scale bar: 100 μm). (F) Protein extracts were prepared from the liver homogenates and subjected to Western blot analysis with antibodies against LC3-II and SQSTM1. Representative Western blot images and the relative quantification of proteins are shown. All data are mean ± SD of at least 3 in vitro and 4–5 in vivo experiments. *$p < 0.05$, **$p < 0.01$. ***p < 0.001.

showed the opposite result. From these results we can understand that the impairment of autophagy by diclofenac is one of the causes of cell death (Fig. S5C). The administration of diclofenac to mice increased the serum ALT, AST and LDH levels in a dose-dependent manner, while pretreatment with rapamycin significantly reduced all the serum biomarkers (Fig. 9D). Histopathology revealed an overall increase in the infiltration of inflammatory cells in the high-dose group. Although individual mice differed in their response, some animals in the high-dose group presented telangiectasis around the portal triad. However, none of the pathological changes mentioned above were observed in the rapamycin pretreatment group (Fig. 9E). Rapamycin-induced reduction in the protein abundance of LC3-II and SQSTM1 was also observed in vivo (Fig. 9F). These data indicate that rapamycin inhibits diclofenac-induced liver injury, which might be related to autophagy activation. In conclusion, diclofenac induces intracellular ROS production and lysosomal dysfunction that lead to the suppression of autophagy. Impaired autophagy fails to maintain mitochondrial integrity and aggravates the cellular ROS burden, which leads to diclofenac-induced hepatotoxicity.

## 3. Discussion

Autophagy is an essential catabolic mechanism for the degradation of cellular components, long-lived cytosolic proteins and damaged organelles in response to a variety of stimuli. The dysregulation of autophagy is linked to a wide range of pathologic conditions induced by diseases, aging and toxic substances [30]. NSAIDs are well tolerated in general, but gastrointestinal tract bleeding is the main concern for the use of these drugs. Other serious adverse effects include kidney and liver toxicity. Diclofenac is the NSAID most frequently reported to induce side effects predominantly related to hepatocellular and cholestatic types of liver injury, which leads to liver failure [31,32]. Diclofenac-induced hepatotoxicity in humans is idiosyncratic. Although the number of toxicological studies on NSAIDs to develop clinically relevant biomarkers and useful therapeutic interventions has increased over the last few decades, the precise mechanism of NSAID-induced hepatotoxicity remains unclear. As reported earlier, the molecular initiating events in diclofenac-induced liver injury are mitochondrial damage and ROS production. Here, we present a critical autophagy-suppressing effect induced by diclofenac and other structurally related NSAIDs, revealing the missing connection between ROS and NSAID-induced liver injury. The key events that determined diclofenac-induced hepatotoxicity were lysosomal dysfunction and autophagic flux impairment mediated by mitochondrial ROS. The lack of efficient degradation of damaged mitochondria by autophagy aggravates cellular oxidative stress and thus induces liver injury (Fig. 10). To the best of our knowledge, this is the first study to demonstrate the causal link between autophagic flux inhibition and hepatotoxicity induced by NSAIDs. The results presented in this study will provide new insight into the molecular mechanisms of NSAID-induced liver injury.

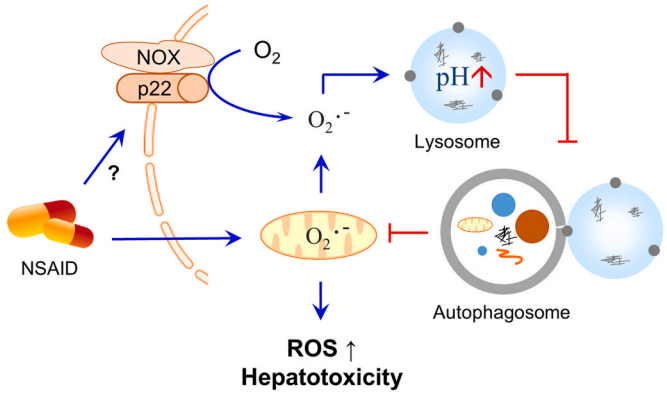


**Fig. 10.** The underlying mechanism of NSAID-induced liver injury. Mitochondrial damage and ROS production induce lysosomal dysfunction and autophagy flux impairment. The failure to efficiently degrade damaged mitochondria by mitophagy induces additional ROS production, leading to hepatotoxicity. See the text for details.

The effects of autophagy on the toxicity of chemicals are not always constant but may vary depending on the cellular context: both cytotoxic and cytoprotective functions have been reported [33]. Autophagy is a kind of cell death. The induction of autophagy in response to anticancer drugs is an example of autophagic cell death, although it represents a cytoprotective mechanism of cells trying to cope with stress [34]. Exposure to some chemicals often leads to autophagic cell death associated with toxicity [35,36]. On the other hand, autophagy is a lysosomal pathway that comprises cellular survival responses to a wide range of stresses, such as nutrient deprivation or chemical insult. Oxidative stress and mitochondrial dysfunction are common mechanisms of a variety of chemical-induced toxicities. Therefore, the selective removal of damaged mitochondria by autophagy is an important protective mechanism that limits the production of additional ROS. A good example is the protection from acetaminophen-induced liver injury by activating autophagy, in which the sustained activation of autophagy attenuates mitochondrial oxidative stress and hepatotoxicity [18,37]. The influences of diclofenac and its metabolites on mitochondrial function are well characterized. Diclofenac induces hepatic mitochondrial dysfunction through several mechanisms: the uncoupling of oxidative phosphorylation and increases in cytosolic calcium and ROS facilitate mitochondrial permeability transition pore opening and the collapse of mitochondrial transmembrane potential followed by ATP depletion [32]. However, signal amplification is required for diclofenac-induced mitochondrial dysfunction to lead to hepatotoxicity. The novel finding of the present study is the presence of a vicious cycle comprising mitochondrial damage, ROS production, autophagy inhibition and damaged mitochondria accumulation to produce additional ROS that leads to hepatotoxicity. More importantly, most of the NSAIDs investigated in this study possess similar properties in terms of ROS production and autophagy inhibition. The results of this study add new insight into the mechanism of mitochondrial damage and hepatotoxicity induced by NSAIDs. Kang et al. aimed to investigate the effects of autophagy induction on diclofenac-induced hepatocyte death; however, the experimental conditions used to induce autophagy with rapamycin were not fully verified and therefore insufficient to be compared with our study [38].

To date, several articles have been published on the effects of NSAIDs on autophagy. Aspirin induces autophagy in colorectal cancer cells by activating AMPK and inhibiting mTOR signaling, which contributes to its protective effects against the development of cancer [39]. Sulindac also induces autophagic cell death in gastric epithelial cells and in lung adenocarcinoma cells by inhibiting Akt/mTOR signaling [40,41]. Celecoxib induces autophagic death in a myeloid leukemia cell line independent of COX-2-inhibitory function [42]. However, some studies have concluded that celecoxib inhibits autophagy based on the data that the drug increases the expression of LC3-II and p62 and inhibits lysosomal function [43]. The effects of indomethacin on autophagy are also inconclusive. Some papers report that indomethacin induces autophagy, while others report the opposite [44,45]. The reasons for the discrepancy may arise from insufficient data and improper interpretation of the results. In some earlier papers describing the effects of NSAIDs on autophagy, the authors drew conclusions only based on very limited biochemical data. Another reason for the inconsistency is the use of inadequate markers for autophagy substrates. Not only diclofenac but also several other NSAIDs induce the autophagy-independent transcriptional upregulation of *sqstm1* and thus the protein level of SQSTM1, which could mislead the interpretation of the results [46]. Therefore, the simple detection of increased LC3-II and SQSTM1 protein levels by NSAIDs does not always indicate the inhibition or induction of autophagy. We therefore used NBR1 expression as a marker for autophagy

substrates rather than SQSTM1 throughout the study. In this study, we provide conclusive data that diclofenac inhibits autophagy in hepatocytes by showing biochemical evidence of autophagic flux and morphological and immunocytochemical characterization of autophagy-related structures, including lysosomes and mitochondria.

The plasma concentration of diclofenac in healthy individuals under therapeutic doses ranged from 2 to 25 μM depending on the dose and route of administration [47,48]. However, it is increased in patients with liver diseases and doubles in patients with hepatic cirrhosis in which first-pass metabolism and biotransformation are substantially compromised [49]. Moreover, some metabolites of diclofenac possess the similar characteristics as diclofenac in terms of the inhibition of autophagy (data not shown). For example, in an overdose case who ingested 1500 mg of diclofenac, the plasma concentration of the unchanged drug went up to about 190 μM [50]. The dose of diclofenac in our animal experiments was also found to be comparable to that in the overdose case if we convert it using the standard body surface area normalization method [51]. Considering the frequent overdose problems, the doses of the drug that we applied in this study is relevant to the acute toxicity of diclofenac.

Next, we explored the mechanism by which diclofenac inhibits autophagic flux. Evidence suggests that ROS modulate autophagy differently depending on the cellular environment. In general, ROS activate autophagy as a survival mechanism to minimize cellular damage. Nutrient starvation induces the production of ROS that directly oxidize and inactivate the delipidation activity of ATG4 on LC3, thus allowing autophagosomes to be elongated correctly [7]. ROS can induce autophagy indirectly via activation of AMPK and inhibition of mTOR, both of which regulate autophagy by the differential phosphorylation of ULK1 [52]. On the other hand, the oxidative stress induced as a result of lysosomal and mitochondrial dysfunction impairs autophagy, which is crucial for oxidative stress-induced cell senescence [14]. The direct oxidation of key autophagy-related proteins ATG3 and ATG7 by ROS inhibits LC3 lipidation and autophagosome formation, which have been reported to be causatively linked to aging and the pathogenesis of many diseases [10]. ROS increase lysosomal pH, which disrupts autophagosome-lysosome fusion and decreases lysosomal cathepsin enzyme activity, leading to the overall impairment of autophagic flux. Autophagosome-lysosome fusion depends on the pH in an acidic compartment of cells [53]. ROS-induced lysosomal dysfunction and thus defective clearance and accumulation of undegraded autophagosomes contribute to neurodegeneration in 1-methyl-4-phenylpyridinium-induced neuronal cells and in Parkinson's disease brain samples [11]. Similar results have been found in esophageal cancer cells treated with ginsenoside. Ginsenoside Ro blocked the autophagosome-lysosome fusion process by increasing lysosomal pH and attenuating lysosomal cathepsin activity, resulting in the accumulation of the autophagosome markers LC3-II and SQSTM1 and the impairment of autophagic flux [15]. These researchers showed that ginsenoside activates NOX associated with the lysosomal membrane and generates ROS locally to increase lysosomal pH. Our results are very similar to those observed in earlier studies demonstrating ROS-induced lysosomal dysfunction and autophagy flux inhibition.

We observed interesting data regarding different effects of rapamycin on diclofenac-induced impairment of autophagy. Experiments of pretreatment with rapamycin demonstrated to be protective of diclofenac toxicity (Fig. 9). However, when rapamycin was treated concomitantly with diclofenac, autophagy was still blocked (Fig. S4). Although the reason for the discrepancy is not fully understood yet, it can be explained by several mechanisms. Autophagy is one of the major routes for the clearance of aggregate-prone proteins or damaged organelles. Therefore, rapamycin treatment facilitates the clearance of abnormal proteins or mitochondria by autophagy and make the cells more resistant to toxic stimuli [54,55]. The protective effects of rapamycin can also be attributed to the regulation of the transcription of genes involved in mitochondrial redox homeostasis, such as RORC1, YY1 and PGC1α [56]. Therefore, rapamycin pretreatment directly inhibits mitochondrial dysfunction and ROS formation in cells under various stress conditions [57,58]. When rapamycin was treated simultaneously with diclofenac, autophagic flux was still suppressed. Under this condition, rapamycin did not have any effect on cellular and mitochondrial ROS production and lysosomal function (Figs. S4B and C). Similar report has been published that the cotreatment of rapamycin with diclofenac did not change cell viability, mitochondrial depolarization and canalicular length, a measure of hepatocyte polarization [38]. Further studies will be needed to ascertain the differences in the rapamycin effects on autophagy depending on the treatment conditions.

One of the key findings of the current study is that diclofenac-induced mitochondrial ROS cause the impairment of lysosomal acidification and consequently lysosomal enzyme activity. The activity of cathepsins B and D determines the efficiency of lysosomal degradation and autophagic flux [59]. We monitored lysosomal integrity by measuring cathepsin B activity directly or using Magic Red reagent, which fluoresces when cleaved in the presence of active cathepsins. We also determined lysosomal acidity using DQ-BSA, a self-quenching fluorescent probe, and LysoSensor Green, a pH-sensitive dye. All the data unequivocally indicate that diclofenac increases lysosomal pH and impairs lysosomal enzyme activity. Moreover, we also found that diclofenac disrupts the fusion of autophagosomes and lysosomes, as shown in data depicting the reduced colocalization of GFP-LC3 with the lysosome membrane marker LAMP1. We also clearly showed that the reactivation of lysosomal activity by clioquinol, a zinc ionophore, or the transfection of TFEB, a transcription factor involved in lysosomal biogenesis, restored autophagic flux. Similarly, scavenging ROS by a general antioxidant, NAC, or a mitochondria-targeted superoxide scavenger, Mito-Tempo, restored lysosomal acidity and autophagic flux in cells treated with diclofenac. The time-course experiments corroborates the results that ROS production and mitochondrial dysfunction precede the lysosomal inactivation (Fig. S12). Another possible mechanism of the defective fusion between autophagosomes and lysosomes could be the disorganization of the Golgi apparatus by diclofenac (unpublished data). Although there is no direct evidence regarding the functional link between the Golgi apparatus and autophagosome-lysosome fusion, the depletion of COPI coat subunits that is required for ER-Golgi transport results in defects in early endosomal function and in the inhibition of autophagic flux [60]. A recent study also demonstrated that CQ impairs the fusion process by disorganizing the Golgi and endolysosomal systems [61]. Further studies are needed to clarify the causal relationship between diclofenac-induced fragmentation of the Golgi and autophagy.

ROS are signaling molecules implicated in the regulation of a variety of cellular processes under normal physiological and pathological conditions. The accumulation of ROS induces oxidative stress, a condition in which cellular macromolecules, including proteins, lipids and DNA, are oxidized and damaged. Therefore, cells have developed enzymatic and nonenzymatic systems to dispose of ROS and to prevent oxidative stress [62]. While the major site of diclofenac-induced hepatic ROS generation is reported to be the mitochondria, NOX also contributes to superoxide production by NSAIDs in different tissues [5,6]. Our data show that the expression of *Nox3* and the NOX-dependent generation of superoxide anions were increased markedly by diclofenac. However, silencing the *Nox3* gene or pretreatment with the Nox3-specific chemical inhibitor ML171 failed to completely restore autophagic activity. As discussed earlier, mitochondria significantly contribute to diclofenac-mediated oxidative stress, increased ROS production and apoptotic cell death. ROS are known to induce lysosomal membrane permeabilization (LMP) by destabilizing lysosomal membrane and inactivating lysosomal enzymes [63]. The crosstalk between the mitochondria and lysosomes are well described in terms of cellular metabolism as well as many key processes such as autophagy, proliferation and cell death. Mitochondrial malfunction induces lysosomal defects either by decreased AMPK signaling or by cellular mediators such as ROS or caspases [64,65]. The cellular responses to lysosomal stress again leads to the perturbations in

communication with mitochondria and suppresses mitochondrial biogenesis and function [66]. Moreover, the release of lysosomal enzymes into the cytosol by LMP activates signaling pathways associated with the lysosomal pathway of apoptosis that has been found to contribute to TNF-α signaling, cholestasis and ischemia-reperfusion injury in the liver [67–69]. Further studies on the functional interdependence between mitochondria and lysosome will provide insight into understanding the NSAID-induced liver injury.

The mitochondrial quality control system is maintained either by fusion/fission dynamics or by mitochondrial turnover via mitophagy. Given the basic role of mitochondrial ROS in virtually all aspects of cellular physiology, the elimination of the source oxidative stress by mitophagy is generally accepted as a kind of cellular defense mechanism to limit the accumulation of ROS and to protect the cell from additional oxidative damage [70]. When mitochondria experience minor stress, they maintain their function by fusion with healthy mitochondria. When they are under additional stress, however, fission is activated to separate the healthy and unhealthy parts of the mitochondria [71]. In the latter case, the subsequent clearance of damaged mitochondria by mitophagy is essential for the completion of the process [72]. In our experiments, we found that the length of mitochondria in the cells treated with diclofenac was significantly reduced. Diclofenac treatment also increased the expression of DRP1 protein, which is responsible for mitochondrial fission, supporting the idea that the cells experience enhanced ROS stimuli. Finally, diclofenac suppressed the basal mitophagy activity that was restored by antioxidants. The impaired removal of damaged mitochondria by mitophagy underlies several hepatic disorders. Impaired mitophagy triggers hepatic NLRP3 inflammasome activation, which contributes to the progression from simple steatosis to steatohepatitis [73]. Aging aggravates hepatic ischemia-reperfusion injury in mice by impairing mitophagy function via insufficient parkin expression [74]. Moreover, defects in mitophagy due to lysosomal cholesterol accumulation increased the susceptibility to hepatotoxicity induced by acetaminophen overdose [75]. Based on these reports, we propose a novel mechanism of diclofenac hepatotoxicity: the primary toxic mechanism of diclofenac is mitochondrial damage and ROS production, as reported previously. Intracellular ROS induce lysosomal dysfunction and autophagy flux impairment that prevent the efficient degradation of damaged mitochondria to limit additional ROS production. The viscous cycle of mitochondrial damage and autophagy impairment aggravate cellular oxidative stress and hepatotoxicity (Fig. 10). The results of this study extend our understanding of the mechanism of hepatotoxicity induced by NSAIDs and provide an approach to managing the liver injury induced by these drugs.

## 4. Materials and methods

### 4.1. Animals

Male C57BL/6 mice (aged 7 weeks) were purchased from the Joongang Animal Laboratory Inc and allowed to acclimate for 1 week at room temperature with a 12:12 h light/dark cycle. The animals were randomly divided into 5 groups (6–9 mice per group). The vehicle group (Veh/Veh) was received intraperitoneally with 0.5% DMSO in saline; diclofenac groups (Veh/Diclo) were administered diclofenac (150 or 200 mg/kg, i.p); rapamycin and diclofenac groups (Rapa/Diclo) were injected with rapamycin (4 mg/kg, i.p) 0.5 h before diclofenac administration. Liver tissues were fixed with 10% neutral-buffered formalin solution embedded in paraffin, and sectioned. Liver sections were stained with hematoxylin and eosin (H&E). All animal experiments were performed in accordance with the guidelines of the Institutional Animal Care and Use Committee of Seoul National University.

### 4.2. Antibodies and reagents

The following primary antibodies were used: anti-LC3B (2775), anti-SQSTM1/p62 (5114), anti-β-Actin (4970), anti-COX2 (12282) and anti-LAMP1 (9091) were purchased from Cell Signaling Technology. Anti-DRP1 (sc271583), anti-NBR1 (sc-130380) and anti-MnSOD (sc-133254) were from Santa Cruz Biochemistry. Anti-COX1 (ab109025) was from Abcam. Goat secondary antibodies to rabbit IgG labelled with Alexa Fluor 546 (A11035), Alexa Fluor 488 (A11034), MitoSOX (M36008), dihydroethidium (DHE; D11347), MitoTracker Red (M7512), LysosensorGreen DND-189 (L7535), DQ-BSA Red (D12051), 3-(4,5-dimethylthiazol-2-yl)-2,5-diphenyltetrazolium bromide (MTT, M6494), 5- (and-6)-chloromethyl-2′,7′-dichlorodihydrofluorescein diacetate (CM-$H_2$DCFDA; C6827) were purchased from Thermo Fisher Scientific. Acetylsalicylic acid (Aspirin, A5376), allopurinol (A8003), diclofenac sodium (D6899) and Mito-Tempo (SML0737) were from Sigma Aldrich. ML171 (4653), and Mito-PY1(4428) were from Tocris Bioscience. Clioquinol (ClioQ; Santa Cruz Biotechnology, sc-201066), Magic Red Assay kit (Immuno Chemistry Technologies, 938), and Annexin-V-FITC and PI kits (BD Biosciences, 556547) were also used.

### 4.3. Cell culture and confluence measurement

HepG2 human hepatoma cells were obtained from ATCC and maintained in Dulbecco's modified Eagle's medium (DMEM; Hyclone, SH30021.01) supplemented with 10% FBS (Gibco, 16000044) and 1% antibiotics-antimycotics (Gibco, 15250062) in humidified air containing 5% $CO_2$ at 37 °C. Mouse primary hepatocyte isolation was performed as described previously [76]. Cell viability was measured using MTT assay. Cell confluency was measured by Cytation 3 cell imaging microplate reader (BioTek). Confluence values were determined from high contrast brightfield images captured every 2 h for 48 h.

### 4.4. Western blot analysis

Cell pellets and liver homogenates were lysed in lysis buffer containing protease inhibitor cocktail (Roche) as described previously [76]. Protein bands were detected with Amersham ECL Prime Detection Reagent (GE Healthcare Life Sciences, RPN2232).

### 4.5. Flow cytometry

For measurement of cellular ROS and mitochondrial ROS levels, detached cells were loaded with CM-$H_2$DCFDA (5 μM), DHE (5 μM), MitoSOX (5 μM) or Mito-PY1 (10 μM), respectively for 20 min at 37 °C. To detect mitochondria and mitochondrial membrane potential, cells were stained with Mitotracker Red (25 nM) and tetramethylrhodamine ethyl ester (TMRE, 100 nM). A FACSCalibur flow cytometer (BD Biosciences) was used for analysis. Relative change in fluorescence was analyzed with FlowJo software.

### 4.6. Identification of oxidized mitochondrial proteins and lipid

Cells were subjected to subcellular fractionation, and the mitochondria-enriched fraction was then lysed in a pH 6.5 buffer containing BIAM, and the resulting lysates were subjected to blot analysis with HRP-conjugated streptavidin or immunoblotted antibodies specific to Prx III as a mitochondrial loading control. To measure the oxidation of mitochondrial cardiolipin, detached cells were incubated with nonyl acridine orange (NAO; Thermo Fisher Scientific, A1372), and then were analyzed by flow cytometry.

### 4.7. Oxygen consumption rate measurement

Oxygen consumption rate (OCR) was measured using Seahorse XFe96 or XFp analyzer (Agilent Technologies) according to the

manufacturer instruction. Cells were treated with oligomycin (1 μM), carbonyl cyanide-4-(trifluoromethoxy)phenylhydrazone (FCCP; 1 μM), and a mixture of antimycin A/rotenone (0.5 μM) for the measurement of key parameters of mitochondrial respiration.

### 4.8. Immunofluorescence analysis and confocal microscopy

Immunofluorescence analysis was performed as described previously [77], with minor modifications. For visualization of the lysosomes, fixed samples were exposed to a blocking solution and then incubated for 30 min at room temperature with antibodies to LAMP1. The cells were washed three times with PBS and then incubated for 30 min at room temperature with Alexa Fluor 488 or 546–conjugated secondary antibodies. For DQ-BSA assay, cells were preloaded with 10 μg/ml DQ-BSA Red in prewarmed medium for 12 h. They were washed with PBS and fixed with 4% paraformaldehyde. For measurement of lysosomal acidity or activity, cells were loaded with Lysosensor Green DND-189 (1 μM) or Magic Red reagent (Immuno Chemistry Technologies) in a prewarmed medium for 1 h after treatment. Then the cells were washed three times with PBS and replaced with phenol red-free DMEM. Images were captured with a Zeiss LSM 880, Nikon A1R or Leica TCS8 confocal microscope. For live mt-Keima imaging, Hep3B cells stably expressing mt-Keima were imaged at two sequential excitations (458 nm, green; 561 nm, red) and 570–695 nm emission range.

### 4.9. Measurement of autophagic flux using tandem fluorescent-tagged LC3

HepG2 cells and MPH seeded in 12-well plates with microscope cover glasses were transfected with GFP-mCherry-LC3 adenovirus for 16 h. After treatment, the cells were fixed with 4% paraformaldehyde and analyzed using confocal microscopy. Autophagy flux was measured by counting the cells with GFP+/mCherry+ (yellow) or GFP-/mCherry+ (red) puncta.

### 4.10. Measurement of cathepsin B activity

Cathepsin B activity was determined by measuring the cleavage of enzyme-specific substrates in whole cell lysates using a commercially available fluorescence-based assay kit (Biovision, K140-100) according to the manufacturer's protocol.

### 4.11. Mitochondrial fragmentation

Cells were incubated with MitoTracker Red or expressed with dsRed-mito, and then confocal microscopic images were analyzed with ImageJ software with MiNA program [27].

### 4.12. Transient transfections

HepG2 cells were transfected with the siRNA duplexes targeting human NOX3 (Bioneer, 50508) or control siRNA using Lipofectamine RNAiMAX (Invitrogen, 13778075). Mouse primary hepatocytes were transfected with siRNA duplexes targeting mouse COX1 (Bioneer, 19224). HepG2 cells were overexpressed with TFEB or MnSOD via transfection of pENTER-CMV-TFEB (Vigene, CH898579) or pCMV-SPORT6-MnSOD (Korean UniGene CloneID hMU001558) using Lipofectamine 2000 (Invitrogen, 11668019). Transfection was performed as described previously [78].

### 4.13. Transmission electron microscopy

Cells were fixed in Karnovsky's buffer for 4 h at 4 °C. They were then post-fixed in 2% osmium tetroxide and 0.1 M cacodylate buffer for 2 h, and embedded in Spurr's resin, sectioned, doubly stained with uranyl acetate, and analyzed using a Zeiss transmission electron microscope.

### 4.14. qRT-PCR analysis

RNA was prepared from cells using Easy-Blue Total RNA Extraction Kit (Intron Biotechnology, 17061). cDNA was synthesized using QuantiTect Reverse Transcription Kit (Qiagen, 205313). The resulting cDNA was amplified by qRT-PCR using iTaq Universal SYBR Green Supermix (Bio-Rad, 1725121). The sequences of primers used for qRT-PCR are listed in Table S1.

### 4.15. Statistical analysis

Experimental data were presented as mean ± S.D. in vivo and in vitro experiments. Data were subjected to student's t-test or one-way ANOVA analysis followed by Turkey's multiple comparison test with GraphPad Prism 7 (GraphPad). P values $< 0.05$ were considered statistically significant.

## Declaration of competing interest

No potential conflict of interest was reported by the authors.

## Acknowledgements

Adenoviral GFP-LC3B and GFP-LC3 were kindly provided by X.M. Yin and J.S. Kim, respectively. Hep3B cells stably expressing Mt-Keima were a gift from J.H. Yun. We thank to B.S. Kim for providing comments about histological analysis.

## Appendix A. Supplementary data

Supplementary data to this article can be found online at https://doi.org/10.1016/j.redox.2020.101751.

## Author contributions

Concept and design of the study: Seung-Hwan Jung, Wonseok Lee, Kang-Yo Lee, You-Jin Choi, Byung-Hoon Lee.

Experiments and procedures of the study: Seung-Hwan Jung, Wonseok Lee, Seung-Hyun Park, Soohee Choi, Dongmin Kang, Sinri Kim, Tong-Shin Chang, Soon-Sun Hong.

Writing of the article: Seung-Hwan Jung, Byun-Hoon Lee.

## Funding

This work was supported by the National Research Foundation of Korea (2020R1A2B5B01001920) and the Ministry of Food and Drug Safety (16173MFDS009) in South Korea.

## References

[1] P.A. Schmeltzer, A.S. Kosinski, D.E. Kleiner, et al., Liver injury from nonsteroidal anti-inflammatory drugs in the United States, Liver Int. 36 (4) (2016) 603–609.
[2] M.J. Gómez-Lechón, X. Ponsoda, E. O'Connor, et al., Diclofenac induces apoptosis in hepatocytes by alteration of mitochondrial function and generation of ROS, Biochem. Pharmacol. 66 (11) (2003) 2155–2167.
[3] H. Al-Attrache, A. Sharanek, A. Burban, et al., Differential sensitivity of metabolically competent and non-competent HepaRG cells to apoptosis induced by diclofenac combined or not with TNF-α, Toxicol. Lett. 258 (2016) 71–86.
[4] M. Syed, C. Skonberg, S.H. Hansen, Mitochondrial toxicity of diclofenac and its metabolites via inhibition of oxidative phosphorylation (ATP synthesis) in rat liver mitochondria: possible role in drug induced liver injury (DILI), Toxicol. Vitro 31 (2016) 93–102.
[5] H. Li, M. Hortmann, A. Daiber, et al., Cyclooxygenase 2-selective and nonselective nonsteroidal anti-inflammatory drugs induce oxidative stress by up-regulating vascular NADPH oxidases, J. Pharmacol. Exp. Therapeut. 326 (3) (2008) 745–753.
[6] M. Domínguez-Luis, A. Herrera-García, M. Arce-Franco, et al., Superoxide anion mediates the L-selectin down-regulation induced by non-steroidal anti-inflammatory drugs in human neutrophils, Biochem. Pharmacol. 85 (2) (2013) 245–256.

[7] R. Scherz-Shouval, E. Shvets, E. Fass, et al., Reactive oxygen species are essential for autophagy and specifically regulate the activity of Atg4, EMBO J. 26 (7) (2007) 1749–1760.
[8] K. Inoki, T. Zhu, K.-L. Guan, TSC2 mediates cellular energy response to control cell growth and survival, Cell 115 (5) (2003) 577–590.
[9] G. Bellot, R. Garcia-Medina, P. Gounon, et al., Hypoxia-induced autophagy is mediated through hypoxia-inducible factor induction of BNIP3 and BNIP3L via their BH3 domains, Mol. Cell Biol. 29 (10) (2009) 2570–2581.
[10] K. Frudd, T. Burgoyne, J.R. Burgoyne, Oxidation of Atg3 and Atg7 mediates inhibition of autophagy, Nat. Commun. 9 (1) (2018) 1–15.
[11] B. Dehay, J. Bové, N. Rodríguez-Muela, et al., Pathogenic lysosomal depletion in Parkinson's disease, J. Neurosci. 30 (37) (2010) 12535–12544.
[12] B.J. Mader, V.N. Pivtoraiko, H.M. Flippo, et al., Rotenone inhibits autophagic flux prior to inducing cell death, ACS Chem. Neurosci. 3 (12) (2012) 1063–1072.
[13] R. Pal, L. Bajaj, J. Sharma, et al., NADPH oxidase promotes Parkinsonian phenotypes by impairing autophagic flux in an mTORC1-independent fashion in a cellular model of Parkinson's disease, Sci. Rep. 6 (2016), 22866.
[14] H. Tai, Z. Wang, H. Gong, et al., Autophagy impairment with lysosomal and mitochondrial dysfunction is an important characteristic of oxidative stress-induced senescence, Autophagy 13 (1) (2017) 99–113.
[15] K. Zheng, Y. Li, S. Wang, et al., Inhibition of autophagosome-lysosome fusion by ginsenoside Ro via the ESR2-NCF1-ROS pathway sensitizes esophageal cancer cells to 5-fluorouracil-induced cell death via the CHEK1-mediated DNA damage checkpoint, Autophagy 12 (9) (2016) 1593–1613.
[16] T. Ueno, M. Komatsu, Autophagy in the liver: functions in health and disease, Nat. Rev. Gastroenterol. Hepatol. 14 (3) (2017) 170.
[17] H.M. Ni, A. Bockus, N. Boggess, et al., Activation of autophagy protects against acetaminophen-induced hepatotoxicity, Hepatology 55 (1) (2012) 222–232.
[18] H.-M. Ni, M.R. McGill, X. Chao, et al., Removal of acetaminophen protein adducts by autophagy protects against acetaminophen-induced liver injury in mice, J. Hepatol. 65 (2) (2016) 354–362.
[19] W.X. Ding, M. Li, X. Chen, et al., Autophagy reduces acute ethanol-induced hepatotoxicity and steatosis in mice, Gastroenterology 139 (5) (2010) 1740–1752.
[20] H.-M. Ni, K. Du, M. You, et al., Critical role of FoxO3a in alcohol-induced autophagy and hepatotoxicity, Am. J. Pathol. 183 (6) (2013) 1815–1825.
[21] X. Chao, S. Wang, K. Zhao, et al., Impaired TFEB-mediated lysosome biogenesis and autophagy promote chronic ethanol-induced liver injury and steatosis in mice, Gastroenterology 155 (3) (2018) 865–879, e12.
[22] B.-R. Seo, S.-J. Lee, K.S. Cho, et al., The zinc ionophore clioquinol reverses autophagy arrest in chloroquine-treated ARPE-19 cells and in APP/mutant presenilin-1–transfected Chinese hamster ovary cells, Neurobiol. Aging 36 (12) (2015) 3228–3238.
[23] R. Ghosh, S.K. Goswami, L.F.B. Feitoza, et al., Diclofenac induces proteasome and mitochondrial dysfunction in murine cardiomyocytes and hearts, Int. J. Cardiol. 223 (2016) 923–935.
[24] A. Panday, M.K. Sahoo, D. Osorio, et al., NADPH oxidases: an overview from structure to innate immunity-associated pathologies, Cell. Mol. Immunol. 12 (1) (2015) 5–23.
[25] L. Li, Q. He, X. Huang, et al., NOX3-derived reactive oxygen species promote TNF-α-induced reductions in hepatocyte glycogen levels via a JNK pathway, FEBS Lett. 584 (5) (2010) 995–1000.
[26] D.P. Singh, S.P. Borse, M. Nivsarkar, Overcoming the exacerbating effects of ranitidine on NSAID-induced small intestinal toxicity with quercetIn: providing a complete GI solution, Chem. Biol. Interact. 272 (2017) 53–64.
[27] A.J. Valente, L.A. Maddalena, E.L. Robb, et al., A simple ImageJ macro tool for analyzing mitochondrial network morphology in mammalian cell culture, Acta Histochem. 119 (3) (2017) 315–326.
[28] H. Katayama, T. Kogure, N. Mizushima, et al., A sensitive and quantitative technique for detecting autophagic events based on lysosomal delivery, Chem. Biol. 18 (8) (2011) 1042–1052.
[29] S.-Y. Choi, J.-S. Park, C.-H. Shon, et al., Fermented Korean red ginseng extract enriched in Rd and Rg3 protects against non-alcoholic fatty liver disease through regulation of mTORC1, Nutrients 11 (12) (2019) 2963.
[30] A.M. Choi, S.W. Ryter, B. Levine, Autophagy in human health and disease, N. Engl. J. Med. 368 (7) (2013) 651–662.
[31] R.A. Thompson, E.M. Isin, Y. Li, et al., In vitro approach to assess the potential for risk of idiosyncratic adverse reactions caused by candidate drugs, Chem. Res. Toxicol. 25 (8) (2012) 1616–1632.
[32] A. Ramachandran, R.G. Visschers, L. Duan, et al., Mitochondrial dysfunction as a mechanism of drug-induced hepatotoxicity: current understanding and future perspectives, Journal of clinical and translational research 4 (1) (2018) 75.
[33] S. Fulda, D. Kögel, Cell death by autophagy: emerging molecular mechanisms and implications for cancer therapy, Oncogene 34 (40) (2015) 5105–5113.
[34] S. Shen, O. Kepp, M. Michaud, et al., Association and dissociation of autophagy, apoptosis and necrosis by systematic chemical study, Oncogene 30 (45) (2011) 4544–4556.
[35] M. Yang, H. Pi, M. Li, et al., From the cover: autophagy induction contributes to cadmium toxicity in mesenchymal stem cells via AMPK/FOXO3a/BECN1 signaling, Toxicol. Sci. 154 (1) (2016) 101–114.
[36] H. Pi, S. Xu, R.J. Reiter, et al., SIRT3-SOD2-mROS-dependent autophagy in cadmium-induced hepatotoxicity and salvage by melatonin, Autophagy 11 (7) (2015) 1037–1051.
[37] M. Yan, L. Ye, S. Yin, et al., Glycycoumarin protects mice against acetaminophen-induced liver injury predominantly via activating sustained autophagy, Br. J. Pharmacol. 175 (19) (2018) 3747–3757.
[38] S.W.S. Kang, G. Haydar, C. Taniane, et al., AMPK activation prevents and reverses drug-induced mitochondrial and hepatocyte injury by promoting mitochondrial fusion and function, PloS One 11 (10) (2016).
[39] F.V. Din, A. Valanciute, V.P. Houde, et al., Aspirin inhibits mTOR signaling, activates AMP-activated protein kinase, and induces autophagy in colorectal cancer cells, Gastroenterology 142 (7) (2012) 1504–1515, e3.
[40] S.-K. Chiou, N. Hoa, A. Hodges, Sulindac sulfide induces autophagic death in gastric epithelial cells via survivin down-regulation: a mechanism of NSAIDs-induced gastric injury, Biochem. Pharmacol. 81 (11) (2011) 1317–1323.
[41] E. Gurpinar, W.E. Grizzle, J.J. Shacka, et al., A novel sulindac derivative inhibits lung adenocarcinoma cell growth through suppression of Akt/mTOR signaling and induction of autophagy, Mol. Canc. Therapeut. 12 (5) (2013) 663–674.
[42] H.-J. Moon, S.-Y. Park, S.-H. Lee, et al., Nonsteroidal anti-inflammatory drugs sensitize CD44-overexpressing cancer cells to Hsp90 inhibitor through autophagy activation, Oncol. Res. 27 (7) (2019) 835–847.
[43] Y. Lu, X.-F. Liu, T.-R. Liu, et al., Celecoxib exerts antitumor effects in HL-60 acute leukemia cells and inhibits autophagy by affecting lysosome function, Biomed. Pharmacother. 84 (2016) 1551–1557.
[44] S. Harada, T. Nakagawa, S. Yokoe, et al., Autophagy deficiency diminishes indomethacin-induced intestinal epithelial cell damage through activation of the ERK/Nrf2/HO-1 pathway, J. Pharmacol. Exp. Therapeut. 355 (3) (2015) 353–361.
[45] J. Vallecillo-Hernández, M.D. Barrachina, D. Ortiz-Masiá, et al., Indomethacin disrupts autophagic flux by inducing lysosomal dysfunction in gastric cancer cells and increases their sensitivity to cytotoxic drugs, Sci. Rep. 8 (1) (2018) 1–10.
[46] D.J. Klionsky, K. Abdelmohsen, A. Abe, et al., Guidelines for the use and interpretation of assays for monitoring autophagy, Autophagy 12 (1) (2016) 1–222.
[47] I. Shah, J. Barker, D.P. Naughton, et al., Determination of diclofenac concentrations in human plasma using a sensitive gas chromatography mass spectrometry method, Chem. Cent. J. 10 (1) (2016) 1–10.
[48] J. Willis, M. Kendall, D. Jack, A study of the effect of aspirin on the pharmacokinetics of oral and intravenous diclofenac sodium, Eur. J. Clin. Pharmacol. 18 (5) (1980) 415–418.
[49] J.S. Lill, T. O'Sullivan, L.A. Bauer, et al., Pharmacokinetics of diclofenac sodium in chronic active hepatitis and alcoholic cirrhosis, J. Clin. Pharmacol. 40 (3) (2000) 250–257.
[50] P. Netter, H. Lambert, A. Larcan, et al., Diclofenac sodium-chlormezanone poisoning, Eur. J. Clin. Pharmacol. 26 (4) (1984) 535–536.
[51] S. Reagan-Shaw, M. Nihal, N. Ahmad, Dose translation from animal to human studies revisited, Faseb. J. 22 (3) (2008 Mar) 659–661.
[52] J. Kim, M. Kundu, B. Viollet, et al., AMPK and mTOR regulate autophagy through direct phosphorylation of Ulk1, Nat. Cell Biol. 13 (2) (2011) 132–141.
[53] A. Kawai, S. Takano, N. Nakamura, et al., Quantitative monitoring of autophagic degradation, Biochem. Biophys. Res. Commun. 351 (1) (2006) 71–77.
[54] Z. Berger, B. Ravikumar, F.M. Menzies, et al., Rapamycin alleviates toxicity of different aggregate-prone proteins, Hum. Mol. Genet. 15 (3) (2005) 433–442.
[55] A. Khan S, F. Salloum, A. Das, et al., Rapamycin confers preconditioning-like protection against ischemia–reperfusion injury in isolated mouse heart and cardiomyocytes, J. Mol. Cell. Cardiol. 41 (2) (2006) 256–264, 2006/08/01/.
[56] J.T. Cunningham, J.T. Rodgers, D.H. Arlow, et al., mTOR controls mitochondrial oxidative function through a YY1-PGC-1alpha transcriptional complex, Nature 450 (7170) (2007 Nov 29) 736–740.
[57] C. Dai, G.D. Ciccotosto, R. Cappai, et al., Rapamycin confers neuroprotection against colistin-induced oxidative stress, mitochondria dysfunction, and apoptosis through the activation of autophagy and mTOR/Akt/CREB signaling pathways, ACS Chem. Neurosci. 9 (4) (2018 2018/04/18) 824–837.
[58] C. Xu, X. Wang, Y. Zhu, et al., Rapamycin ameliorates cadmium-induced activation of MAPK pathway and neuronal apoptosis by preventing mitochondrial ROS inactivation of PP2A, Neuropharmacology 105 (2016 2016/06/01/) 270–284.
[59] U. Repnik, V. Stoka, V. Turk, et al., Lysosomes and lysosomal cathepsins in cell death, Biochim. Biophys. Acta Protein Proteonomics 1824 (1) (2012) 22–33.
[60] M. Razi, E.Y. Chan, S.A. Tooze, Early endosomes and endosomal coatomer are required for autophagy, JCB (J. Cell Biol.) 185 (2) (2009) 305–321.
[61] M. Mauthe, I. Orhon, C. Rocchi, et al., Chloroquine inhibits autophagic flux by decreasing autophagosome-lysosome fusion, Autophagy 14 (8) (2018) 1435–1455.
[62] R. Scherz-Shouval, Z. Elazar, Regulation of autophagy by ROS: physiology and pathology, Trends Biochem. Sci. 36 (1) (2011) 30–38.
[63] T. Kurz, A. Terman, B. Gustafsson, et al., Lysosomes in iron metabolism, ageing and apoptosis, Histochem. Cell Biol. 129 (4) (2008) 389–406.
[64] L. Fernandez-Mosquera, K.F. Yambire, R. Couto, et al., Mitochondrial respiratory chain deficiency inhibits lysosomal hydrolysis, Autophagy 15 (9) (2019 2019/09/02) 1572–1591.
[65] C.M. Deus, K.F. Yambire, P.J. Oliveira, et al., Mitochondria-lysosome crosstalk: from physiology to neurodegeneration, Trends Mol. Med. 26 (1) (2020 Jan) 71–88.
[66] K.F. Yambire, L. Fernandez-Mosquera, R. Steinfeld, et al., Mitochondrial biogenesis is transcriptionally repressed in lysosomal lipid storage diseases, Elife (2019 Feb 18) 8.
[67] M.E. Guicciardi, J. Deussing, H. Miyoshi, et al., Cathepsin B contributes to TNF-alpha-mediated hepatocyte apoptosis by promoting mitochondrial release of cytochrome c, J. Clin. Invest. 106 (9) (2000) 1127–1137.
[68] A. Canbay, M.E. Guicciardi, H. Higuchi, et al., Cathepsin B inactivation attenuates hepatic injury and fibrosis during cholestasis, J. Clin. Invest. 112 (2) (2003 Jul) 152–159.
[69] X. Zhang, J.J. Lemasters, Translocation of iron from lysosomes to mitochondria during ischemia predisposes to injury after reperfusion in rat hepatocytes, Free Radic. Biol. Med. 63 (2013) 243–253, 2013/10/01/.

[70] G. Filomeni, D. De Zio, F. Cecconi, Oxidative stress and autophagy: the clash between damage and metabolic needs, Cell Death Differ. 22 (3) (2015) 377–388.
[71] R.J. Youle, A.M. Van Der Bliek, Mitochondrial fission, fusion, and stress, Science 337 (6098) (2012) 1062–1065.
[72] G. Ashrafi, T. Schwarz, The pathways of mitophagy for quality control and clearance of mitochondria, Cell Death Differ. 20 (1) (2013) 31–42.
[73] N.-P. Zhang, X.-J. Liu, L. Xie, et al., Impaired mitophagy triggers NLRP3 inflammasome activation during the progression from nonalcoholic fatty liver to nonalcoholic steatohepatitis, Lab. Invest. 99 (6) (2019) 749–763.
[74] Y. Li, D-y Ruan, C-c Jia, et al., Aging aggravates hepatic ischemia-reperfusion injury in mice by impairing mitophagy with the involvement of the EIF2α-parkin pathway, Aging 10 (8) (2018) 1902.
[75] A. Baulies, V. Ribas, S. Núñez, et al., Lysosomal cholesterol accumulation sensitizes to acetaminophen hepatotoxicity by impairing mitophagy, Sci. Rep. 5 (2015) 18017.
[76] K.-Y. Lee, W. Lee, S.-H. Jung, et al., Hepatic upregulation of fetuin-A mediates acetaminophen-induced liver injury through activation of TLR4 in mice, Biochem. Pharmacol. 166 (2019) 46–55.
[77] S. Park, J.M. Lim, S.H. Park, et al., Inactivation of the PtdIns(4)P phosphatase Sac1 at the Golgi by H2O2 produced via Ca(2+)-dependent duox in EGF-stimulated cells, Free Radic. Biol. Med. 131 (2019 Feb 1) 40–49.
[78] K.-Y. Lee, S. Oh, Y.-J. Choi, et al., Activation of autophagy rescues amiodarone-induced apoptosis of lung epithelial cells and pulmonary toxicity in rats, Toxicol. Sci. 136 (1) (2013) 193–204.